PCT WORLD INTELLECTUAL PROPERTY ORGANIZATION
International Bureau

INTERNATIONAL APPLICATION PUBLISHED UNDER THE PATENT COOPERATION TREATY (PCT)

(51) International Patent Classification 6 : F16L 9/14 | A1

(11) International Publication Number: **WO 99/08033**

(43) International Publication Date: 18 February 1999 (18.02.99)

(21) International Application Number: PCT/US97/13342

(22) International Filing Date: 22 July 1997 (22.07.97)

(71) Applicant: EXXON RESEARCH AND ENGINEERING COMPANY [US/US]; 180 Park Avenue, P.O. Box 390, Florham Park, NJ 07932-0390 (US).

(72) Inventors: MONETTE, Liza; 10 Westchester Terrace, Annandale, NJ 08807 (US). CHIU, Allen, S.; 8 Rustic Court, Florham Park, NJ 07932 (US). MUELLER, Russell, R.; Apartment 507, 507 Washington Gardens, Washington, NJ 07882 (US). ANDERSON, Michael, P.; 10 Westway, Clinton, NJ 08809 (US).

(74) Agents: HANTMAN, Ronald, D. et al.; Exxon Research and Engineering Company, P.O. Box 390, Florham Park, NJ 07932-0390 (US).

(81) Designated States: AU, CA, JP, NO, European patent (AT, BE, CH, DE, DK, ES, FI, FR, GB, GR, IE, IT, LU, MC, NL, PT, SE).

Published
With international search report.

(54) Title: HIGH WEEPING STRENGTH POLYMER-GLASS RIBBON COMPOSITE LAMINATES FOR FLUID CONTAINMENT

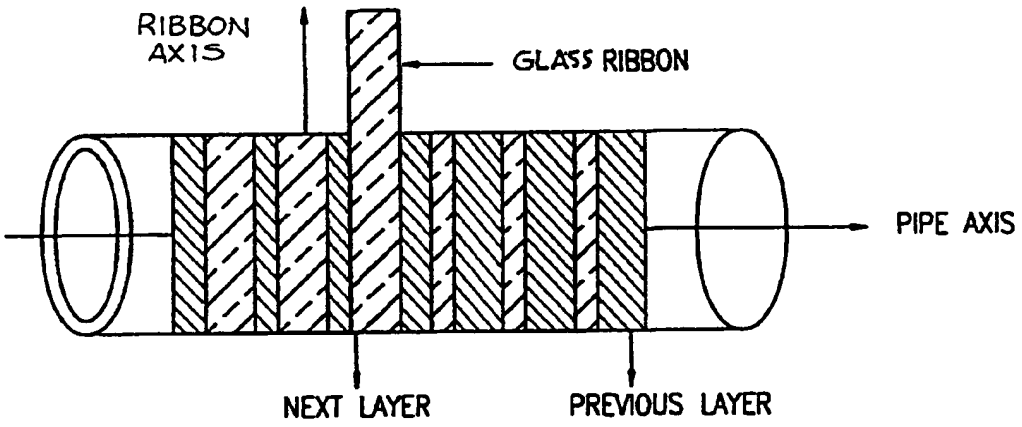

(57) Abstract

The present invention is a high weeping strength polymer-glass ribbon composite laminate for fluid containment. The laminate includes a reinforced composite tubular body which comprises a tubular polymeric matrix including a thermosetting polymer with tensile elongation to break less than 25 % and a glass ribbon reinforcement embedded within said tubular polymeric matrix. The reinforcing ribbon may be helically wound at an angle between 0-90 with respect to the pipe axis, or wound at an angle of about 90° with respect to the pipe axis.

FOR THE PURPOSES OF INFORMATION ONLY

Codes used to identify States party to the PCT on the front pages of pamphlets publishing international applications under the PCT.

AL	Albania	ES	Spain	LS	Lesotho	SI	Slovenia
AM	Armenia	FI	Finland	LT	Lithuania	SK	Slovakia
AT	Austria	FR	France	LU	Luxembourg	SN	Senegal
AU	Australia	GA	Gabon	LV	Latvia	SZ	Swaziland
AZ	Azerbaijan	GB	United Kingdom	MC	Monaco	TD	Chad
BA	Bosnia and Herzegovina	GE	Georgia	MD	Republic of Moldova	TG	Togo
BB	Barbados	GH	Ghana	MG	Madagascar	TJ	Tajikistan
BE	Belgium	GN	Guinea	MK	The former Yugoslav Republic of Macedonia	TM	Turkmenistan
BF	Burkina Faso	GR	Greece			TR	Turkey
BG	Bulgaria	HU	Hungary	ML	Mali	TT	Trinidad and Tobago
BJ	Benin	IE	Ireland	MN	Mongolia	UA	Ukraine
BR	Brazil	IL	Israel	MR	Mauritania	UG	Uganda
BY	Belarus	IS	Iceland	MW	Malawi	US	United States of America
CA	Canada	IT	Italy	MX	Mexico	UZ	Uzbekistan
CF	Central African Republic	JP	Japan	NE	Niger	VN	Viet Nam
CG	Congo	KE	Kenya	NL	Netherlands	YU	Yugoslavia
CH	Switzerland	KG	Kyrgyzstan	NO	Norway	ZW	Zimbabwe
CI	Côte d'Ivoire	KP	Democratic People's Republic of Korea	NZ	New Zealand		
CM	Cameroon			PL	Poland		
CN	China	KR	Republic of Korea	PT	Portugal		
CU	Cuba	KZ	Kazakstan	RO	Romania		
CZ	Czech Republic	LC	Saint Lucia	RU	Russian Federation		
DE	Germany	LI	Liechtenstein	SD	Sudan		
DK	Denmark	LK	Sri Lanka	SE	Sweden		
EE	Estonia	LR	Liberia	SG	Singapore		

HIGH WEEPING STRENGTH POLYMER-GLASS RIBBON COMPOSITE LAMINATES FOR FLUID CONTAINMENT

BACKGROUND/PRIOR ART

This invention relates to polymer-glass ribbon composite laminates for fluid containment. In particular, this invention relates to a modification to the reinforcement morphology of polymer-glass fiber composite laminates designed to increase the strength and longevity of pressure containing devices made from such laminates (under static pressure) and fatigue performance (under cyclic pressure). The invention has utility for oil and gas production/transmission applications. Pressure containing devices include: pipes, downhole tubulars, pipelines, pressure vessels, underground storage tanks. Other applications include composite wraps and crack arrestors. Containment pressure can be increased from current commercially available levels up to 5000 psig long term service pressure. The performance of pressure containing devices is limited by poor mechanical properties of the individual laminates, in the direction normal to the fiber axis. It has been found that the use of glass ribbons having aspect ratio between 10 and 1000 in the direction normal to the ribbon axis (e.g. ribbon or tape morphology) as reinforcement results in increases to normal stiffness and strength of the composite laminate providing an enhancement in containment capability.

Pressure containing devices (such as pipes, downhole tubulars, underground storage tanks, pressure vessels, pipelines, wraps and crack arrestors) fabricated from epoxy-fiber glass composites are increasingly used in oil and gas production. For instance, low pressure piping in entire fields are being upgraded to take advantage of these materials. The benefits of composites over equivalent metal structures primarily involve their superb corrosion resistance, leading to a decreased life-cycle cost. Other attractive advantages include their high strength and stiffness per unit weight, flexibility in material design, and improved fatigue resistance.

Nevertheless, polymer composites as presently supplied contain a serious deficiency that precludes their use in applications that generate even moderate stress levels. Although the composite material exhibits an axial strength (in the fiber direction) of up to 200 ksi (with pristine glass fibers), 100 ksi (for non-pristine glass fibers) the device exhibits a loss of fluid containment integrity referred to as weeping, by which

matrix microcracking and ply delamination provide a leak path for the fluid at short and long term service pressures which are an order of magnitude less than the burst pressure.

For composite pipes, the microcracking can be alleviated by increasing the pipe wall thickness. However, this solution drives the composite pipe cost up by approximately 30% as compared to that of carbon steels (for example, a 2000 psi pressure, 2-7/8" outside diameter downhole tubing). This higher cost constitutes a barrier to the substitution of composite pipes for carbon steels in low pressure applications (i.e. flow lines). Composite pipes have not as yet been introduced in more demanding, higher pressure functions (pipelines), as the cost of increasing further the wall thickness becomes prohibitive.

Similarly, composites used as downhole tubulars do not compete favorably against the more expensive corrosion resistant alloys (CRAs). The required wall thickness of composite tubulars prevents their use in many applications where the diameter of the hole connecting the oil in geologic formation to the surface is constrained. Other devices such as composite underground storage tanks also exhibit premature microcracking, hence their corrosion resistance does not offer any additional advantages over similar metal structures. Matrix microcracking occurring in composite wraps considerably reduces their longevity (for construction/rejuvenation applications), as moisture eventually diffuses through the resulting cracks and directly attacks the glass, thereby weakening the reinforcement.

Therefore, there is a need for material having increased containment capacities particularly for moderate to high pressure piping/tubing in production and transmission of fluids such as oil and gas.

The polymer matrix in these composite pipes is typically a thermosetting system, e.g. an epoxy, which solidifies by cross-linking (chemical reaction). Thermoplastic systems can also be envisioned as an acceptable material. The matrix in this case solidifies by a physical phenomenon such as crystallization from the melt. The cross-linked thermosetting plastic has a Young's modulus around 430 ksi, and a tensile strength between 11-13 ksi and a tensile elongation to failure less than 25%. Continuous glass reinforcement (currently fibers with a diameter 15μm, volume fraction 60%) are embedded in a mixture of thermosetting resin and curing agent. The mixture is initially uncured, so its viscosity is usually low enough (few hundreds cp) to ensure

reasonable wetting of the glass reinforcement by the mixture. To make a tubular, the resulting ply is wound around a mandrel, at an angle between 0° and 90° with respect to the pipe axis. In the example shown in Figure 1, the winding angle θ is 55°, and the laminate is viewed in a direction along the fiber length or axis. The winding angle θ is then tilted to 125° (or -55°) upon reaching the end of the mandrel, then back to 55° and so on. Several winding angles can be used in this process, i.e. 0, ±45° and ±70°. The resulting pipe is referred to as a multidirectional filament wound pipe. The pipe is subsequently heat treated, so the thermosetting resin can solidify by cross-linking. The result is a pipe, referred to as filament wound pipe, with inside diameter typically ranging from 1" to 36" and wall thickness from 0.1" to 2.0". Common pipe dimensions consists of 4" inside diameter and 0.16" wall thickness.

Figure 2 shows a short-term failure envelope, i.e. fluid containment limits due to matrix micro-cracking, weeping, measured for a representative composite pipe with fiber/matrix parameters and dimensions as described in the paragraph above, under different petrochemical service conditions: 1. Pure axial stress; 2. Hoop stress equal to axial stress (downhole tubulars); 3. Hoop stress twice the axial stress (surface pipes); and 4. Pure hoop stress (buried pipes). The service pressure can be obtained by dividing the value of the hoop strength on the graph by the ratio R/T (inside radius over the wall thickness) and by a service factor of 4 to account for visco-elastic relaxation of matrix (static pressure), or matrix fatigue behavior (cyclic pressure) for long-term service (20 years). For instance, such a pipe used as a downhole tubular can withstand a service pressure of 500 psig; used as a surface pipe, a service pressure of 1500 psig; and used as a buried pipe, a service pressure of 1000 psig.

SUMMARY OF THE INVENTION

The present invention is a high weeping strength polymer-glass ribbon composite laminate for fluid containment. The laminate includes a reinforced composite tubular body which comprises a tubular polymeric matrix including a thermosetting polymer with tensile elongation to break less than 25% and a glass reinforcing strip or ribbon embedded within said tubular polymeric matrix. The reinforcing strip may be helically wound about the longitudinal axis of said tubular body or wound at an angle between –90° and 90° with respect to the pipe axis.

In a preferred embodiment, the axial Young's modulus of the tubular body is greater than 50% of the rule of mixture value.

Brief Description of the Drawings

Figure 1 shows an example of a reinforced tube with the winding at an angle of 55°. The fiber volume fraction is 60%. The reinforcement illustrated consists of conventional glass fibers.

Figure 2 shows a failure envelope with containment limits for matrix micro-cracking and weeping.

Figure 3 shows the stresses induced by gas or fluid pressure in the wall of a typical epoxy-based pipe. The winding angle is 55°.

Figure 4 shows the relationships in the coarse-grained spring model used in the present invention. Central node (i) and eight (8) mechanically interacting neighbors (j), (k), (l), (m), (n), (o), (p) and (q). k_{ij} is the spring constant between two nearest neighbors, and k_{ik} is the spring constant between two next-nearest neighbors. c_{ijk} is the bond bending constant, shown here between bonds ij and ik. All equilibrium angles between two bonds, i.e. $\Theta_{ijk} = \Theta_{ikl} = \Theta_{ilm} = \Theta_{imn} = \Theta_{ino} = \Theta_{iop} = \Theta_{ipq} = \Theta_{ipj} = \Theta_o = \pi/4$.

Figure 5 shows the stress-strain plot according to the simulation model applied to a typical laminate with conventional glass fibers having a volume fraction of 58%. The strain ε is applied in the direction normal to the fiber axis, according to the simulation model.

Figure 6a shows a schematic of a metal ribbon/epoxy pipe.

Figure 6b shows a cross-section of the pipe wall of Figure 6a.

Figure 7 shows E_N as a function of s/s_c for a fixed ratio $E_R/E_m = 24$. Aspect ratios $s < s_c$ are not desirable because of poor load transfer properties. Aspect ratios $s > 5s_c$ may compromise the ease of processing, even though load transfer is close to ideal.

Figures 8a and 8b show a glass ribbon composite pipe and wall cross-section for a ribbon distribution with $\ell = L/2$ and $L_o = L/4$.

Figures 9a and 9b show a glass ribbon composite pipe and wall cross-section for a ribbon distribution with $l < 0.02$ L and $L_o = L/2$.

Figures 10a and 10b show a glass ribbon composite pipe and wall cross-section for a random distribution of reinforcement.

Figure 11a shows a short-term failure envelope of invention, a glass ribbon/epoxy pipe (full circles, dashed line), as compared to failure envelope of current ±55° glass fiber/epoxy pipe (full squares, full line). The ribbons have aspect ratio L/t = 170 (L and t are the ribbon width and thickness, respectively) and they are wound at 90° (i.e. around the pipe circumference). The ribbon distribution is ordered, with an overlap parameter $L_o = L/5$ and distance between adjacent ribbon edges $\ell < L/10$.

Figure 11b shows a long-term failure envelope of invention, a glass ribbon/epoxy pipe (full circles, dashed line), as compared to failure envelope of current ±55° glass fiber/epoxy pipe (full squares, full line). The ribbons have aspect ratio L/t = 170 (L and t are the ribbon width and thickness, respectively) and they are wound at 90° (i.e. around the pipe circumference). The ribbon distribution is ordered, with an overlap parameter $L_o = L/5$ and distance between adjacent ribbon edges $\ell < L/10$.

Figure 12a shows a short-term failure envelope of invention, a glass ribbon/epoxy pipe (full circles, dashed line), as compared to failure envelope of current ±55° glass fiber/epoxy pipe (full squares, full line). The ribbons have aspect ratio L/t = 170 (L and t are the ribbon width and thickness, respectively) and they are wound at 90° (i.e. around the pipe circumference). The ribbon distribution is random.

Figure 12b shows a long-term failure envelope of invention, a glass ribbon/epoxy pipe (full circles, dashed line), as compared to failure envelope of current ±55° glass fiber/epoxy pipe (full squares, full line). The ribbons have aspect ratio L/t = 170 (L and t are the ribbbon width and thickness, respectively) and they are wound at 90° (i.e. around the pipe circumference). The ribbon distribution is random.

Detailed Description of the Invention

The detailed description of the invention shall be discussed according to the following outline:

I. Relationship Between Service Pressure and Laminate Normal Strength
II. Simulation Model
III. Comparison of the Present Invention with the Prior Art
IV. Implementation of the Invention
  A. Invention Principles
  B. Important Composite Parameters For Optimized Composite Laminate Transverse Properties of Invention
  C. Selection Guidelines and Range of Values For Composite Parameters Leading to Optimized Transverse Composite Laminate Properties of Invention
    1. Ordered Ribbon Distributions
      a. Distance Between Ribbons, $\ell > 0.1L$
      b. Distance Between Ribbons, $\ell \leq 0.1L$
      c. Composite Transverse Laminate Weeping Strength
      d. Selection Criteria/Range of Values
    2. Random Ribbon Reinforcement Distribution
      a. Critical Aspect Ratio For Random Ribbon Distribution
      b. Transverse Laminate Tensile Weeping Strength
      c. Selection Criteria/Range of Values
V. Example: Projected Performance of Invention
  A. Ordered Ribbon Distribution
  B. Random Ribbon Distribution
VI. Glass Ribbon Fabrication

I. Relationship Between Axial Weeping Failure of Pipe And Laminate Normal Strength

The stresses induced by gas/fluid pressure in the wall of a typical epoxy-based pipe using conventional glass fibers are shown on fig. 3. A pipe under pressure can experience hoop, axial and radial stresses. Both the hoop and axial stresses are

tensile in nature, while the radial stress σ_r is compressive and can usually be neglected because it is small compared to the other two. These three stresses are shown acting on a small volume element of laminate, on lower left of fig. 3, where the reinforcement, e.g. conventional fibers or glass ribbons are wound at 55° angle to the pipe axis. We now focus on the axial and hoop stresses only. The axial stress is given by:

$$\sigma_z = PR^2 / (2RT + T^2) \tag{1}$$

in the case of a pipe with closed ends. P is the fluid pressure, R is the inner pipe radius and T the pipe wall thickness. The hoop stress is given by Barlow's equation[4] for a service pressure less than 1000 psig:

$$\sigma_\theta = PR / T \tag{2}$$

and by a thick wall approximation[4], for a service pressure greater than 1000 psig:

$$\sigma_\theta = P(2R^2 + 2RT + T^2) / (2RT + T^2) \tag{3}$$

Both these stresses can be resolved into longitudinal, normal and shear stress components, with respect to a reference frame where one of the direction (L) coincides with the reinforcement axis (for a single conventional laminate):

$$\sigma_L = \sigma_\theta \sin^2\theta + \sigma_z \cos^2\theta \tag{4}$$

$$\sigma_N = \sigma_\theta \cos^2\theta + \sigma_z \sin^2\theta \tag{5}$$

$$\tau = (\sigma_\theta - \sigma_z)\cos\theta \sin\theta \tag{6}$$

where (N) is a direction perpendicular to the (L) direction, and the winding angle θ = 55°, as can be seen on the lower right fig. 4. According to eqs (4) and (5), σ_L is comparable to σ_N, for service conditions 2, 3 and 4 on fig. 2. The strength in the direction along the reinforcement axis (L) is controlled by the reinforcement strength, and is approximately 60 ksi. However, the strength in the direction normal to the reinforcement axis (N) is controlled by the matrix strength in the case of conventional fibers. The resulting laminate short-term normal strength will be shown below to be less

than 10 ksi for conventional fibers. Hence premature pipe failure is initiated by microcracking of the matrix in between the fibers for conventional composites due to either matrix visco-elastic relaxation (static pressure) or fatigue (cyclic pressure) arising from loading in the normal direction. Note that the shear stress is not considered here. Shear stress arise from the loading in the longitudinal and normal directions, due to the fact the reinforcement is helically would around the pipe body at an angle Θ different than 0° or 90°. The shear stress can be engineered away by appropriate choice of the winding angle, i.e. $\Theta = 90°$.

The axial failure stress on fig. 2 can be related to the normal laminate strength by a simple analysis using eq. (5) and setting σ_θ to 0:

$$\sigma_z = \sigma_N / \sin^2 \theta \qquad (7)$$

The normal laminate strength σ_N may be deduced from eq. (7), using the empirical axial failure stress of 11.25 ksi for conventional fiber-composites (point 1 on fig. 2), and its value is 7.5 ksi for 60% fiber content. This value will be used later for computer model validation.

The above analysis is based on a single ply and ignores the laminate shear modulus and strength. It can be shown that a more detailed analysis based on an angle-ply laminate (i.e. layers at ±55°), and taking into account laminate shear properties yields a transverse tensile strength of 7 ksi, in agreement with this simpler analysis.

2. Simulation Model

A model methodology is introduced here and will be used to demonstrate the concept on which the invention is based: A ribbon-like reinforcement morphology increases the amount of load transfer, hence the ply strength in the direction normal to the reinforcement axis.

The elastic properties of the simulation model have been described elsewhere (L. Monette, M. P. Anderson, H. D. Wagner and R. R. Mueller, J. Appl. Phys. 76 (1994) 1442) (L. Monette and M. P. Anderson, Modelling Simul. Mater. Eng. 2 (1994) 53), and will be briefly mentioned here. The simulation model is a coarse-grained spring model on a two dimensional lattice of dimensions 200 x 200, with spring

constants $k_{\alpha\beta}$ and bond bending constants $c_{\alpha\beta\gamma}$. Each of the 40000 nodes interacts with four nearest neighbors (i.e. connected by bonds $\alpha\beta$ = ij, il, in and ip on fig. 4) and with four next-nearest neighbors (i.e. connected by bonds $\alpha\beta$ = ik, im, io and iq on fig. 4). $r_{\alpha\beta}$ is the distance between nodes α and β, and the equilibrium bond length, $r_{\alpha\beta}^{\circ} = a_o$ for a nearest neighbor bond and $r_{\alpha\beta}^{\circ} = \sqrt{2}a_o$ for a next-nearest neighbor bond. $\Theta_{\alpha\beta\gamma}$ is the angle between bonds $\alpha\beta$ and $\alpha\gamma$, and the equilibrium angles $\Theta_{\alpha\beta\gamma} = \Theta_{ijk} = \Theta_{ikl} = \Theta_{ilm} = \Theta_{imn} = \Theta_{ino} = \Theta_{iop} = \Theta_{ipq} = \Theta_{iqj} = \Theta_o = \pi/4$. The constants $k_{\alpha\beta}$ and $c_{\alpha\beta\gamma}$ are defined as follows: $k_{\alpha\beta} = 2k_g$ if the nodes α and β are nearest neighbor glass nodes and $k_{\alpha\beta} = k_g$ if α and β are next-nearest neighbor glass nodes; $k_{\alpha\beta} = 2k_m$ if the nodes α and β are nearest neighbor matrix nodes and $k_{\alpha\beta} = k_m$ if α and β are next-nearest neighbor matrix nodes; $k_{\alpha\beta} = 2k_i$ if the nodes α and β are nearest neighbor glass and matrix nodes and $k_{\alpha\beta} = k_i$ if α and β are next-nearest neighbor glass and matrix nodes. $c_{\alpha\beta\gamma} = c_m$ if bonds $\alpha\beta$ and $\alpha\gamma$ are matrix bonds. $c_{\alpha\beta\gamma} = c_g$ if bonds $\alpha\beta$ and $\alpha\gamma$ are glass bonds. $c_{\alpha\beta\gamma} = c_i$, if bonds $\alpha\beta$ and $\alpha\gamma$ are a matrix and glass bonds, or a glass and matrix bonds, respectively. The interface elastic constants are chosen such that $k_i = k_m$ and $c_i = c_m$. The energy V_{ij} stored in a bond between nodes i and j is:

$$V_{ij} = \tfrac{1}{2}k_{ij}(r_{ij} - r_{ij}^{\circ})^2 + 1/2\sum c_{\alpha\beta\gamma}(\cos\Theta_{\alpha\beta\gamma} - \cos\Theta_o)^2 \qquad (11)$$

where r_{ij} is the distance between nodes i andj, and upon the application of a strain, $r_{ij} \neq r_{ij}^{\circ}$. The summation in the second term on the right hand side of (11) is over angles $\alpha\beta\gamma$=ijk, ijq, jil, and jip, and upon application of a strain, $\Theta_{\alpha\beta\gamma} \neq \Theta_o$. The matrix or glass (m,g) Young's modulus and Poisson ratio are given by the following expressions:

$$E_{m,g} = 8k_{m,g}[k_{m,g} + (c_{m,g}/a_o^2)]/[3k_{m,g} + (c_{m,g}/a_o^2)] \qquad (12)$$

$$v_{m,g} = [k_{m,g} - (c_{m,g}/a_o^2)]/[3k_{m,g} + (c_{m,g}/a_o^2)] \qquad (13)$$

The constants $k_m = 285$ ksi, $c_m = 28$ ksi a_o^2, $k_g = 6428$ ksi, $c_g = 1071$ ksi a_o^2 are chosen, such that the matrix has Young's modulus of 428 ksi and Poisson ratio 0.3 (typical of a cured thermosetting resin used in fiber-reinforced pipes), and that the glass has Young's modulus of 10285 ksi and Poisson ratio 0.2.

Periodic boundary conditions are used in the direction of applied tensile strain or stress, while free boundary conditions are applied in the other direction. Mechanical equilibrium of the system is ensured by a conjugate gradient technique. The present simulation model incorporates a failure criterion via the cohesive energy parameter U_{ij}. The bond between node i and j is broken if it accumulates an energy V_{ij} greater than its assigned cohesive energy U_f for a glass bond, U_i for an interface bond and U_m for a matrix bond, and $U_i = U_m$. The parameters $U_m = 0.14$ ksi and $U_g = 1.71$ ksi have been chosen such that the matrix tensile strength is 13 ksi, and the glass tensile strength is 100 ksi. These values are typical for thermosetting resins and for glass reinforcement, respectively. The tensile elongation of the matrix at break is less than 0.25, for example, 0.03. Tensile elongation is defined as change in length over original length, $\frac{\Delta \ell}{\ell}$.

The model is subsequently used to simulate the stiffness and strength of a conventional glass fiber laminate, in the direction normal to the fiber axis.

The poor loading of the reinforcement in the direction normal to the fiber axis implies that the laminate strength in that direction is matrix-dominated, as the matrix always exceeds its tensile failure criterion first. The fibers can be viewed in that direction as two dimensional particles which do not carry a load significantly greater than that of the matrix. Furthermore, when close enough to one another, they act as stress raisers, causing stress amplifications in the matrix material. Therefore, the occurrence of failure is expected at a value of external applied stress much less than the strength value of the pure matrix material. The normal laminate strength is usually less than the strength of the pure matrix materials, hence the empirical value of 7.5 ksi deduced in 1. above for a 60% reinforcement volume fraction is less than the strength 13 ksi for the pure matrix material.

Figure 5 is a stress/strain curve obtained from the model for a conventional laminate with a fiber volume fraction of 58%, typical of the laminates used for pipe fabrication. The normal laminate strength is 8 ksi, a value within 7% of the empirical value of 7.5 ksi. It is therefore concluded that the model yields conventional glass fiber laminate normal strength in good agreement with that of a real conventional glass fiber laminate.

III. Comparison of the Present Invention with the Prior Art

Strip (or ribbon) reinforced composites are known in the art see US patent 3,790,438, to provide enhanced mechanical properties, but are limited to polymers with a tensile elongation greater than 25%. The reason given for this strain limitation is that the matrix material must have sufficient elongation to decrease the effect of stress concentrations due to thermal stresses arising during the manufacturing process.

Metal strip reinforced tubular body, in which the matrix (typically a thermoset) has a tensile elongation less than 25% have recently been proposed see US patent 4,657,049. The invention is described as providing a tubular body comprised of a thermosetting polymer in which metallic reinforcing strips are completely embedded such that the entire load borne by the polymer is distributed to the reinforcing strips. In consequence, the advantages of the invention are claimed to be such that it:

(i) Provides a tubular body with high mechanical strength, i.e. burst strength, and high stiffness,
(ii) Provides corrosion resistance,
(iii) Can be manufactured on large scale at low cost,

and is therefore claimed to be suited for the conduction of wide variety of gases, liquids, slurries, solid particulates and other materials.

Neither US patent 3,790,438, nor US patent 4,657,049 provide any teaching for improving the resistance to loss of fluid containment arising from microcracking or leaks in these materials for the following reasons:

(i) US patent 3,790,438 limits the range of validity of their invention (strip reinforced composites) to polymeric matrices with tensile elongation equal or greater than 25%. The polymeric material typically used in composite pipes for oil/gas applications is a thermoset, which has a tensile elongation less than 25%. Therefore, US patent 3,790,438 does not teach how to improve mechanical properties of composites where the matrix has a tensile elongation less than 25%.

(ii) US patent 4,657,049 claims that metal strip reinforced composites display an improvement in mechanical properties, such as burst strength and stiffness. However, for the particular problem of pipe leakage, burst strength is irrelevant. The pipes never burst upon occurrence of weeping, or loss of containment. The US patent 4,657,049 claims of an increased burst strength and stiffness enabling the conduction of highly pressurized fluids is probably justified. The internal pressure which a reinforced composite tubular body of given diameter can resist (without bursting) obviously depends upon the mechanical strength of the reinforcing strips, hence the use of metal strips. However, the caveat is that in the oil fields, loss of containment integrity occurs at pressures which are well below the internal pressure needed to cause the conventional fiber-reinforced pipes to burst. In fact, there is no mention of matrix microcracking, weeping, or containment integrity in the wording of US patent 4,657,049. In consequence, there is no teaching provided in US patent 4,657,049 which clearly demonstrates that one should expect an improved burst strength or improved stiffness to increase the pipe containment integrity (weeping resistance) as well.

The following is simulation data generated by the model described in section 2. The purpose is to demonstrate the above argument (ii), i.e. that increasing the reinforcement strength and stiffness may greatly increase the pipe burst strength and stiffness, but does not improve the leaking resistance significantly above that of the conventional fiberglass/epoxy pipes. Let a pipe be made by winding metal strips coated with epoxy, so the strip axis is perpendicular to the pipe axis, as shown in fig. 6a. Each turn or convolution of strip (of width L and thickness t) in one layer overlaps two turns or convolutions of strip in adjacent layers, and is also offset with respect to these adjacent turns by a length L_O, as shown in fig. 6b of a tubular wall cross-section (strip axis pointing out of the page).

The offset length L_O is at the minimum equal to $L_C/2$, and L_C is given by $L_C = t\,\sigma_R/(2\tau_i)$, where σ_R is the tensile strength of the reinforcement, τ_i is the shear strength of the interface between the reinforcement and the polymeric matrix, and t is the strip thickness. The following table is based on the two first rows of the table in US patent 4,657,049. We have added the tensile weeping strength σ_w, and ($\sigma_w = \sigma_N$ because the pipe longitudinal axis is perpendicular to the reinforcement axis) at which the US patent 4,657,049 invention, a metal strip reinforced pipe, displays loss of fluid containment; the tensile strength σ_d where matrix microcracking first occurs (and $\sigma_d <$

σ_w), leading eventually to loss of fluid containment; and E_N, the laminate Young's modulus in the direction normal to reinforcement axis. σ_w, σ_d and E_N are calculated from our simulation model, with the following parameters taken from US patent 4,657,049:

Reinforcement (Metal 1 in US patent 4,657,049)
Tensile strength: $\sigma_R = 90 kg/mm^2 = 126$ ksi
Young's modulus: $E_R \sim 20 \times 10^3 kg/mm^2 = 28571$ ksi
Volume fraction of reinforcing strips: $v_f = 50\%$
Ribbon thickness: t=0.1mm

Matrix (Epoxy A in US patent 4,657,049)
Tensile strength: $\sigma_m \sim 2 kg/mm^2 = 2.8$ ksi(Deduced from pipe hoop strength: $\sigma_\theta = v_f \sigma_R + (1-v_f)\sigma_m = 46 kg/mm^2$)
Young's modulus: $E_m \sim 0.25 \times 10^3 kg/mm^2 = 357$ ksi (Deduced from pipe hoop modulus: $E_\theta = v_f E_R + (1 - v_f)E_m \sim 10 \times 10^3 kg/mm^2$)

Interfacial shear strength: $\tau_i = 1.5 kg/mm^2 = 2.1$ ksi
Critical ribbon width: $L_C = t\,\sigma_R/(2\tau_i) = 3$mm

Table 1 compares the expected pipe axial strength: $\sigma_Z = fv_f\sigma_R + (1 - fv_f)\sigma_m$, (and $f = 1-L_O/L$) as predicted in US patent 4,657,049, to the weeping strength σ_w, ($\sigma_w = \sigma_N$) and stress σ_d at which first damage occurrence begins, as determined by the computer model:

Table 1

Ribbon Width L (mm)	Ribbon Aspect Ratio	Offset Length L_O (mm)	$f=1-L_O/L$	σ_Z (ksi)	σ_w (ksi)	σ_d (ksi)	E_N (ksi)
16	160	4	0.75	49	15	9	7714
40	400	4	0.90	59	16	6	10571

The following four conclusions can be drawn from the data in Table 1:

The tensile weeping resistance σ_w of US patent 4,657,049 metal strip reinforced tubular, as measured by the simulation model described in section 2 is 3 to 4 times less than the predicted pipe axial strength σ_Z. Therefore, the pipe tensile weeping

strength σ_w, which is the pipe usable strength before occurrence of loss of containment, is a property independent of the pipe ideal axial strength σ_Z.

The axial weeping strength σ_w ($\sigma_w = \sigma_N$) of US patent 4,657,049 metal strip reinforced tubular has not been increased significantly above that of conventional ± 55° filament wound fiberglass/epoxy pipes, which is σ_w = 11.2 ksi (and $\sigma_w \neq \sigma_N$, for 3.89" inside diameter and 0.16" wall thickness); and is below that of commercially available multidirectional filament wound fiberglass/epoxy pipes, which is σ_w = 21.4 ksi (and $\sigma_w \neq \sigma_N$, for 1.94" inside diameter and 0.23" wall thickness).

There is no teaching in US patent 4,657,049 on how to select reinforcement and matrix properties to increase the weeping resistance above what is currently provided by commercial composite tubular goods, up to the theoretical limit of $\sigma_w = \sigma_Z$ (in table 1).

The tensile stress level σ_d at which matrix microcracking first appears as determined by the simulation model for the US patent 4,657,049 metal strip reinforced tubular is 0.5 to 0.8 lower than the tensile weeping strength of conventional ±55° filament wound fiberglass/epoxy pipes. This implies that US patent 4,657,049 metal strip reinforced tubular is likely to loose its corrosion resistance at service pressures where state of the art composite pipes/tubulars provide corrosion resistance. The initial matrix microcracking encountered at these lower tensile strengths provides an entry path for the corrosive fluids present in petrochemical applications to attack and progressively degrade the metal reinforcement.

IV. Implementation of the Invention

A. Invention Principles

We have indicated in section I that (in the absence of shear stresses), the weeping resistance of current composite pipes is limited by the laminate transverse strength. The principle on which the present invention is based is that the load transfer in the direction normal to the reinforcement axis must be increased, in order to increase the laminate transverse strength, hence the composite resistance to weeping. An approach to increase load transfer is to modify the reinforcement morphology, i.e. from cylindrical to ribbon-like, as to increase the surface area in the transverse direction. This

increased surface area is expected to give rise to shear tractions, which lead to increased reinforcement loading in the laminate transverse direction. The reinforcement has a ribbon-like cross-section made of bulk glass, such that it possesses a normal aspect ratio (ratio of ribbon width over thickness) much greater than one. For example, in order to obtain a ribbon aspect ratio of 170, given a ribbon thickness of 15μ, the required ribbon width is 2.5 mm. A stress field analysis indicates that the load transfer in the normal direction from the matrix to the reinforcement has been greatly improved. For example, the average stress transferred to the reinforcement in the direction along the ribbon width can be three times higher than that transferred to the same volume fraction of reinforcement with cylindrical morphology, i.e. fibers (see Section II). The average stress carried by the matrix is consequently three times less than that carried by the matrix for a cylindrical reinforcement (see Section II). The load transfer from the matrix to the reinforcement now occurs by a shear-lag mechanism (H. L. Cox, Br. J. Appl. Phys. 3 (1952) 72), i.e. by shear tractions along the ribbon width at the reinforcement/matrix interface. Therefore, both the laminate Young's modulus and strength in the direction normal to the fiber axis are expected to increase significantly above the matrix value.

B. Important Composite Parameters For Optimized Composite Laminate Transverse Properties Of Invention

The composite parameters which may influence the laminate transverse strength (in case of a ribbon-like reinforcement morphology) are: E_R (reinforcement Young's modulus), E_m (matrix Young's modulus), ratio s/s_c (where s is the ribbon transverse aspect ratio and s_c the ribbon transverse critical aspect ratio), τ_i (interface shear strength), σ_m (matrix tensile strength) and v_f (the reinforcement volume fraction). The ribbon laminate normal strength is given by:

$$\sigma_N = E_N \cdot \varepsilon_N^* \tag{13}$$

where

$$E_N = \Theta(E_R, E_m, s/s_c, v_f) \tag{14}$$

is the ribbon laminate transverse Young's modulus. Θ is a function which will be described below, and

$$\varepsilon_N^* = \Xi(E_R, E_m, s/s_c, \tau_i, \sigma_m, v_f^{min}) \quad (15)$$

is the ribbon laminate transverse failure strain. Ξ is an undetermined function. v_f^{min} will be described in section C, paragraph 1.

It can also be shown (L. Monette, M. P. Anderson and G. S. Grest, J. Appl. Phys. 75 (1994) 1155) that the ribbon laminate normal modulus can be related to the average reinforcement transverse tensile strain:

$$E_N = v_f(E_R - E_m)(\varepsilon_R)_N/(\varepsilon_a)_N + E_m \quad (16)$$

With the use of shear lag analysis, it can be demonstrated that the average ribbon laminate transverse tensile strain $(\varepsilon_R)_N$ is related to the ribbon dimensions:

$$\frac{(\varepsilon_R)_N}{(\varepsilon_a)_N} = \left(1 - \frac{s_c}{2s}\right) \quad (17a)$$

and $s_c = L_c/t$, the critical aspect ratio, with t = ribbon thickness diameter, and L_c the critical ribbon width; L is the ribbon width; and $(\varepsilon_a)_N$ is the applied transverse tensile strain. Equation (17a) implies that when $s = s_c$,

$$(\varepsilon_R)_N / (\varepsilon_a)_N = 1/2 \quad (17b)$$

therefore, one obtains

$$E_N = v_f(E_R - E_m)(1 - s_c/2s) + E_m \quad (18)$$

Figure 7 is a plot of E_N as a function of s/s_c for a fixed ratio $E_R/E_m = 24$ (i.e. a glass ribbon/epoxy system). E_N tends asymptotically to the rule of mixture value $E_{RM} = v_f(E_R - E_m) + E_m$ as the ribbon transverse aspect ratio $s \rightarrow \infty$. The rule of mixtures defines the maximum property level (here E_{RM}) a multi-component structure can possess, based on the property level of the individual components (E_R, E_m), averaged on the basis of their respective volume fraction, or concentration.

The expression given for the critical metal ribbon transverse aspect ratio s_c in US patent 4,657,049, namely:

$$s_c = \sigma_R/(2\tau_i) \tag{19}$$

suggests that the same composite performance can be achieved by decreasing the interfacial shear strength by a factor of two, say, and increasing the critical ribbon transverse aspect ratio by a factor of two simultaneously. This is true for ribbon aspect ratios less than or of order s_c, where the transverse composite modulus variation is approximately linear with the ribbon transverse aspect ratio s, (see fig. 7 such that a decrease in composite transverse failure strain by roughly a factor of 2 (due to the decrease in the interfacial shear strength by a factor of 2) can be compensated by a factor of 2 increase in the composite transverse modulus obtained by increasing the ribbon transverse aspect ratio s. Therefore, the transverse composite strength given in eq. (13) remains unchanged. However, in the limit $s > s_c$ (which is the meaningful limit to composite design), this is no longer true. The transverse composite modulus dependence on ribbon transverse aspect ratio is almost flat in this limit, as can be seen on fig. 7. Therefore, the increase in transverse modulus can no longer compensate for the drop in transverse composite failure strain. Hence, the transverse composite strength in eq. (13) is expected to be less than ideal. This is one of the reasons for the low weeping resistance of the US patent 4,657,049 invention, as measured by our computer model in Table 1. The reinforcement tensile strength σ_R as proposed by US patent 4,657,049 is not a relevant parameter to the design of the ribbon reinforcement transverse aspect ratio.

The three most important composite parameters for this invention are: 1) s_c, the transverse ribbon critical aspect ratio

$$s/s_c = \Phi(E_R, E_m, v_f) \tag{20}$$

where Φ is a function which depends on the ribbon distribution, and will be further described in the section 4.3. s is the ribbon transverse aspect ratio, and should be selected once s_c is known, such that the transverse ribbon laminate modulus in eq. (18) can be optimized, i.e. to be increased as close to ideal limit. Once the parameters E_R, E_m, v_f and s/s_c are set, the important composite parameters to maximize the transverse

failure strain are obtained from eq. (15), i.e. 2) the interfacial shear strength τ_i and 3) matrix tensile strength σ_m. Range of values for both will also be given in section 4.3.

C. Selection Guidelines And Range of Values For Ribbon Composite Parameters Leading to Optimized Transverse Composite Laminate Properties of Invention

1. Ordered Ribbon Distributions

This distribution is better suited for ribbons whose thickness is of order 0.1mm, and width that can reach several cm. Those ribbons can be directly wound onto the mandrel (preferable at an angle of 90° with respect to pipe axis so shear stresses are eliminated), and not increase pipe processing costs (in this case, $\sigma_w = \sigma_N = \sigma_Z$).

Firstly, let us show that the tensile weeping strength of a ribbon composite pipe improves, when the efficiency of load transfer, the interfacial shear strength and the matrix strength are increased. Let us consider a ribbon-like glass reinforcement/epoxy system with the following properties:

Reinforcement:
Tensile strength: σ_R = 100 ksi (assuming same strength as convention glass fibers)
Young's modulus: E_R = 10286
Reinforcement failure strain ε_R^* = 3.0%
Volume fraction of reinforcing strips: v_f = 50%
Ribbon thickness: t=0.1mm

The matrix is an epoxy, typically used for filament wound pipes for petrochemical applications, with the following properties:

Tensile strength: σ_m = 13 ksi
Young's modulus: E_m = 428 ksi
Failure strain: ε_m^* = 0.03

Interfacial shear strength: τ_i= 6.4 ksi. The interfacial shear strength for a glass/epoxy system has been estimated from fragmentation experiments.

Table 2 shows the tensile weeping strength σ_w and ($\sigma_w = \sigma_Z = \sigma_N$) of a pipe made with glass ribbon laminates , as compared to the tensile weeping strength of the US patent 4,657,049 pipe (taken from table 1), where the reinforcement lay-up is kept the same (see fig. 6a and b).

Table 2

Ribbon Width L (mm)	Ribbon Aspect Ratio	Offset Length L_0 (mm)	f=1-L_0/L	σ_w (ksi) Metal	E_N (ksi) Metal	σ_w (ksi) Glass	E_N (ksi) Glass
16	160	4	0.75	15	7714	34.5	4428
40	400	4	0.90	16	10571	34.5	5000

Three conclusions can be drawn from table 2:

i. The tensile weeping strength of the present invention is 2.3 times greater than the tensile weeping strength of the US patent 4,657,049 invention, both determined by the simulation model. Using eq. (18) and the results for E_N from table 2, $s_c \sim 160$ for the metal ribbon and $s_c \sim 40$ for the glass ribbon. The load transfer efficiency is therefore greater for glass than metal ribbons, where the ribbon aspect ratios selected (i.e. 160 and 400) are only 1 to 2 times greater that the critical aspect ratio for the metal ribbon reinforcement, while the same ribbon aspect ratio is 4 to 10 times greater than the critical aspect ratio when the ribbon is made out of bulk glass . The greater load transfer efficiency, together with increased interfacial shear strength and matrix strength explains the greater tensile weeping strength of the current invention, as compared to US patent 4,657,049 invention.

ii. Ribbon aspect ratios 4 to 5 times the critical aspect ratio seem to be optimal, as the results in table 3 for the glass ribbon reinforcement shows no difference in the tensile weeping strength between the ribbon with aspect ratio 160 and 400.

iii. The US patent 4,657,049 claim that the metal ribbon pipe has greater stiffness than the state of the art composite pipes is correct.

We will consider ordered distributions of the following type: Let ℓ be the distance separating two axially adjacent ribbons of width L (this distance is unspecified

in US patent 4,657,049), and L_O is the length by which a layer is offset with respect to the radially adjacent layers. Both ℓ and L_O can obey the following relations:

$$1) \qquad 0.5 \le 1 - \frac{L_O}{L} \le 0.9 \qquad \ell \le 0.1L \tag{21a}$$

$$2) \qquad L = \ell + 2L_O \qquad\qquad \ell \ge 0.1L \tag{21b}$$

and L is the ribbon width.

Figures 8a and 8b illustrates a ribbon composite pipe and wall cross section which has a ribbon distribution for with $\ell = L/2$ and $L_O = L/4$, while figs. 9a and 9b illustrates a ribbon composite pipe and wall cross section which has a ribbon distribution with $\ell \le 0.1L$ (i.e. as small as possible), and $L_O \sim L/2$. Note that the lowest volume fraction v_f^{min} achievable with distribution (21a) (see fig. 8b) or distribution (21b) (fig. 9b) is

$$v_f^{min} = (1 - \frac{L_O}{L})\, v_f, \tag{22}$$

for $L_o = L/2$, $v_f^{min} = v_f/2 \left(1 - \frac{L_O}{L}\right)$ should be > 0.5, ideally around 0.75, to maximize v_f^{min}, $v_f^{min} = \frac{3}{4} v_f$. Ribbon distributions with $\ell \sim 0$ and $0.9 \le 1 - L_O/L \le 1.0$ as proposed in US patent 4,657,049 are rejected because they lead to a high ribbon transverse critical aspect ratio, i.e. they do not optimize load transfer, especially for modulus ratios $E_R/E_m > 50$. For instance, the transverse modulus data (E_N) in table 1 together with eq. (18) yields $s_c = 160$ for f=0.75 and s_c=225 for f=0.9. Assuming a design criterion $s \sim 2s_c$ for the ribbon transverse aspect ratio, this means that the ribbon width to ensure strengthening for overlap $L/L_O > 0.9$ is greater than 45 cm, assuming a thickness of 0.1 mm.

The following quantifies the dependence of the ribbon critical aspect ratio on the reinforcement /matrix modulus ratio E_R/E_m, and the reinforcement volume fraction v_f, for reinforcement lay-ups as described by eqs. (21a and 21b). The extreme cases $\ell = L/2$ and $\ell \sim 0$ will be examined explicitly.

a. Distance Between Ribbons, $\ell > 0.1L$ (i.e. $\ell = L/2$)

Tables 3, 4 and 5 make use of same matrix/interface parameters as for table 2.

Table 3

E_R/E_m=24

v_f=33%

s	E_N (ksi)
24	1186
50	2028
90	2586
170	3028
340	3243
680	3329

The data is best fitted by a modification of eq. (18), i.e.

$$E_N = v_f(E_R - E_m)[1-(s_c/2s)^{\mu}]+E_m \qquad (23)$$

with s_c = 40 and μ=0.727.

Table 4

E_R/E_m=70

v_f=33%

s	E_N (ksi)
24	1371
50	2986
90	4714
170	6971
340	8285
680	8814

By fitting the data of table 4 with the help of eq. (23), we obtain $s_c = 85$ and $\mu=0.739$.

Table 5

$E_R/E_m=100$

$v_f=33\%$

s	E_N (ksi)
24	1386
50	3214
90	5500
170	8986
340	11271
680	12271

By fitting the data of table 5 with the help of eq. (23), we obtain $s_c = 105$ and $\mu=0.728$. An average value $\mu=0.73$ is determined from the results.

Therefore, the dependence of the ribbon laminate critical transverse aspect ratio can be written as:

$$s_c \sim [E_R/E_m)/(E_R/E_m)_{ref}]^{\nu} (s_c)_{ref}(v_f) \qquad (24)$$

With $E_R/E_m)_{ref} = 24$ (glass/epoxy is reference system), $(s_c)_{ref}(v_f = 33\%) = 40$ and $\nu = 0.69$. The dependence of $(s_c)_{ref}$ with v_f is then evaluated, and the results are shown in table 6

Table 6

v_f	s_c
0.33	40
0.67	35

According to the results shown in table 6, the volume fraction of reinforcement does not seem to influence the value of the ribbon critical transverse aspect ratio, therefore $(s_c)_{ref}(v_f) = (s_c)_{ref} = 40$.

b. Distance Between Ribbons, $\ell \leq 0.1L$ (i.e. $\ell = 0.02L$)

Tables 7, 8 and 9 make use of same matrix/interface parameters as for table 2.

Table 7

E_R/E_m=24

v_f=50%

s	E_N (ksi)
24	1900
50	3086
90	3814
170	4486
340	4900
680	5128

The data is fitted using eq. (23), with s_c = 50 and μ=0.937.

Table 8

E_R/E_m=70

v_f=50%

s	E_N (ksi)
24	2343
50	4843
90	7300
170	10400
340	12500
680	13743

By fitting the data of table 8 with the help of eq. (23), we obtain $s_c = 95$ and $\mu=0.913$.

Table 9

$E_R/E_m = 100$

$v_f = 50\%$

s	E_N (ksi)
24	2428
50	5314
90	8600
170	13371
340	16814
680	18914

By fitting the data of table 9 with the help of eq. (23), we obtain $s_c = 125$ and $\mu=0.880$. An average value $\mu=0.91$ is determined from the results.

Therefore, the dependence of the ribbon laminate critical transverse aspect ratio can be written as:

$$s_c \sim [(E_R/E_m)/(E_R/E_m)_{ref}]^{\nu} (s_c)_{ref}(v_f) \qquad (25)$$

With $(E_R/E_m)_{ref} = 24$ (glass/epoxy is reference system), $(s_c)_{ref}(v_f = 50\%)$ and $\nu = 0.62$. The dependence of $(s_c)_{ref}$ with v_f is then evaluated, and the results are shown in table 10

Table 10

v_f	s_c
0.33	48
0.50	50

According to the results shown in table 10, the volume fraction of reinforcement does not seem to influence the value of the ribbon critical transverse aspect ratio, therefore $(s_c)_{ref}(v_f) = (s_c)_{ref} = 50$.

c. Composite Transverse Laminate Weeping Strength

Once the ribbon transverse aspect ratio is chosen so the transverse Young's modulus to rule of mixture prediction ($E_{RM} = v_f E_R + (1 - v_f)E_m$) ratio is 50% or more, the only way to increase the composite transverse laminate weeping strength is either to increase the interfacial shear strength, or choose a system with a high interfacial shear strength such as glass/epoxy system. Table 11 shows the composite transverse Young's modulus E_N, the average transverse tensile strain transferred to the reinforcement $\langle\varepsilon_R\rangle_N$ normalized to the applied strain $(\varepsilon_a)_N$, the laminate transverse tensile weeping strength ($\sigma_w = \sigma_N = \sigma_Z$) and transverse tensile failure strain ε_N^* for a ribbon lay-up ($\ell = L/2$, $L_O = L/4$ for example) and volume fraction $v_f = 0.67$ ($v_f^{min} = 0.33$) (see fig. 8a and 8b), with the same reinforcement/matrix/interface parameters used for table 2:

Table 11

s	E_N (ksi)	$\langle\varepsilon_R\rangle_N/\varepsilon_a$	σ_w (ksi)	ε_N^* (%)
24	2628	0.34	26.5	1.0
50	4371	0.60	39.4	0.9
90	5243	0.73	50.4	1.0
170	5857	0.85	51.4	0.9
340	6128	0.87	55.1	0.9
680	6257	0.91	50.1	0.8

Glass ribbons with aspect ratio $s \geq 2s_c$ will impart to the invention an axial weeping strength superior to the state of the art composite pipes made with conventional glass fibers. For example, in the above table, a glass ribbon of aspect ratio 90 will result in a pipe with axial weeping strength $\sigma_w = \sigma_N = \sigma_Z = 50.4$ Ksi. The invention axial weeping strength is 4.5 times stronger than currently available ±55° filament wound pipes, and 2.4 times stronger than currently available multidirectional filament wound pipes.

d. Selection Criteria/Ranges of values

For a given reinforcement to matrix Young's modulus ratio E_R/E_m, the critical ribbon transverse aspect ratio can be determined by eq. (24) for lay-ups with $0.1L < \ell < L/2$; and by eq. (25) for lay-ups with $\ell < 0.1L$. Comparing Equation (23) yields the average tensile strain transferred to the reinforcement, and normalized to the applied strain, i.e. $\frac{(\varepsilon_R)_N}{(\varepsilon_a)_N} = [1 - (s_c / 2s)^{\mu}]$, with $\mu = 0.73$ and s_c from eq. (24) for lay-ups with $0.1L < \ell < L/2$; or with $\mu = 0.91$ and s_c from eq. (25) for lay-ups with $\ell < 0.1L$. Note that the lay-up with $\ell \sim L/2$ is expected to yield a slightly greater transverse laminate tensile weeping strength than any other lay-up $\ell < L/2$. This is because at fixed volume fraction, the ribbon ends are closer to the strain field of the ribbons in the adjacent layer, thereby minimizing the stress concentrations at the ribbon tips.

Reinforcement volume fraction should be in the range $0.4 \leq v_f \leq 0.8$, preferably in the range $0.5 \leq v_f \leq 0.7$.

The average tensile strain transferred to the reinforcement should be at least greater than 50% of the applied strain with preferred value around 80%. Therefore this requires a ribbon transverse aspect ratio $s > 4.5\ s_c$ for lay-ups with $0.02L < \ell < L/2$, while $s > 3s_c$ for lay-ups with $\ell < 0.02L$.

The modulus ratio E_R/E_m could assume any value, but the higher its value, the higher is the interfacial shear strength needed to ensure increased laminate transverse strength. We feel a range $20 < E_R/E_m < 100$ is reasonable, with the load transfer efficiency being optimum for E_R/E_m closer to the lower limit of 20.

The interfacial shear strength should ideally have a value of τ_i= 6 ksi or higher. An interfacial shear strength less than that will reduce the transverse laminate tensile strength increase of the invention as compared to state of the art composite pipes. We do not recommend interfacial shear strengths lower than about 3 ksi, especially for reinforcements with a high modulus ratio E_R/E_m. For $E_R/E_m > 50$, we recommend an interfacial shear strength around 6 ksi, or greater.

The matrix tensile strength should not be below the value for the interfacial shear strength, i.e. $\sigma_m \geq \tau_i$

2. Random Ribbon Reinforcement Distribution

Figure 10 illustrate the present invention, a ribbon laminate wound pipe with winding angle between 0 and 90° with respect to pipe axis. The next layer of laminate is wound at an angle opposite in magnitude (sign) to the pipe axis in the preceding layer, although not necessarily the exact opposite degree of winding angle. On fig. 10a, the winding angle is ±90°, as an example. Note that the laminate shear stress vanishes. Figure 10b is a cross-sectional view of a laminate made of a random arrangement of ribbon-like reinforcement. This distribution would be appropriate for ribbon-like reinforcement which is very thin, t < 0.05mm and narrow. The laminate thickness should not be less than 0.1mm, so the manufacturing costs of the invention do not increase.

a. Critical Aspect Ratio For Random Ribbon Distribution

In tables 13 to 16, the glass reinforcement and matrix possess the same tensile strength and Young's modulus and the matrix /interface properties are the same as used for table 2, with :

Volume fraction of reinforcing strips: $v_f = 50\%$
Ribbon thickness: t=0.015mm

Table 13

s	E_N (ksi)
24	1500
50	2471
90	3214
170	4057
340	4686

Data in table 13 is fitted using eq. (23), with s_c =90 and μ = 1.

In order to establish a functional relation between s_c and the reinforcement to matrix modulus ratio E_R/E_m, and the volume fraction of reinforcement v_f, we have determined the ribbon critical aspect ratio for several modulus ratios and fixed volume fraction (table 14); as well as for several volume fractions and fixed modulus ratio (table 15).

Table 14

$v_f = 50\%$

E_R/E_m	s_c
24	90
70	175
100	220

The results of table 14 can be fitted by the following functional relationship:

$$s_c \sim [(E_R/E_m)(E_R/E_m)_{ref}]^{v} (s_c)_{ref}(v_f) \qquad (26)$$

$(E_R/E_m)_{ref} = 24$ (glass/epoxy is reference system), and $(s_c)_{ref}(v_f = 50\%) = 90$. Table 15 helps to quantify how the critical ribbon transverse aspect ratio for the reference system varies with the volume fraction of reinforcement:

Table 15

$E_R/E_m = 24$

$v_f(\%)$	s_c
40	99
50	90
60	75

The results of table 15 can be fitted by the following functional relationship:

$$(s_c)_{ref}(v_f) = 150\,(-2v_f^2 + 1.2v_f + 0.5) \qquad (27)$$

b. Transverse Ribbon Laminate Tensile Weeping Strength

Table 16 shows the composite transverse Young's modulus E_N, the average transverse tensile strain transferred to the reinforcement $\langle\varepsilon_R\rangle_N$ normalized to the applied strain $(\varepsilon_a)_N$, the laminate transverse tensile weeping strength ($\sigma_w = \sigma_N$) and transverse tensile failure strain ε_N^* for glass ribbons distributed randomly (see fig. 10a and b) and volume fraction $v_f = 0.50$. The reinforcement /matrix /interface parameters are the same as the ones used for table 2.

Table 16

Ribbon aspect ratio(s)	E_N (GPa)	$(\varepsilon_R)_N/(\varepsilon_a)_N$	σ_w (MPa)	ε^*_N (%)
24	1500	0.22	9.0	0.65
50	2471	0.41	11.7	0.50
90	3214	0.56	14.0	0.50
170	4057	0.74	20.6	0.55
340	4686	0.86	34.0	0.75

Glass ribbons with aspect ratio 4 times or more the critical aspect ratio will impart to the invention an axial weeping strength superior to the state of the art composite pipes. For example, in table 16, a glass ribbon of aspect ratio 340, wound at 90° (fig. 10a and b), will result in a pipe with axial weeping strength $\sigma_w = \sigma_N = 34$ ksi. The invention axial weeping strength is 3 times stronger than currently available ±55° filament wound pipes, and 1.6 times stronger than currently available multidirectional filament wound pipes. If pipe is wound at ±55° with glass ribbon of same aspect ratio, the resulting axial weeping strength $\sigma_w = 34/\sin^2 55° = 51$ ksi (with $\sigma_w \neq \sigma_N$). The invention axial weeping strength is now 4.6 times stronger than currently available ±55° filament wound pipes, and 2.4 times stronger than currently available multidirectional filament wound pipes.

c. Selection Criteria/Ranges of Values

The critical ribbon transverse aspect ratio can be determined by eqs (26) and (27). The ribbon aspect ratio should be at least 4 to 5 times greater than the critical aspect ratio.

The modulus ratio E_R/E_m could assume any value, but the higher its value, the higher the interfacial shear strength is needed to ensure increased laminate transverse strength. We feel a range $20 < E_R/E_m < 100$ is reasonable, with the load transfer efficiency being optimum for E_R/E_m closer to the lower limit.

Reinforcement volume fraction should be in the range $0.4 \leq v_f \leq 0.8$, preferably in the range $0.5 \leq v_f \leq 0.7$.

The interfacial shear strength should ideally have a value of $\tau_i = 6$ ksi or higher. An interfacial shear strength less than that will reduce the transverse laminate tensile strength increase of the invention as compared to state of the art composite pipes. We do not recommend interfacial shear strengths lower than about 2 ksi, especially for reinforcements with a high modulus ratio E_R/E_m. For $E_R/E_m > 50$, we recommend an interfacial shear strength around 6 ksi, or greater.

The matrix tensile strength should not be below the value for the interfacial shear strength, i.e. $\sigma_m \geq \tau_i$

V. Example: Projected Performance of Invention

A. Ordered Ribbon Distribution ($\ell \sim 0$ and $L_O = L/5$)

New short-term failure envelope is shown on fig. 11a for a pipe fabricated with ribbon-like glass reinforcement with aspect ratio s=170 and volume fraction $v_f = 50\%$, as compared to current state of the art. In this case, the glass ribbon have tensile strength $\sigma_R^* = 200$ ksi, while the matrix and interface properties are the same as for Table 2. The failure criterion used here is based on the von Mises failure criterion (D. Hull, "An Introduction to Composite Materials", Cambridge University press, (1981) p. 169) which was originally applied to homogeneous and isotropic bodies, then expanded and modified by Hill to anisotropic bodies, and applied to composite materials by Tsai:

$$(\sigma_L/\sigma_L^*)^2 + (\sigma_N/\sigma_N^*)^2 + (\tau/\tau^*)^2 = 1 \qquad (28)$$

In this case, $\sigma_L^* = 100$ ksi,
$\sigma_N^* \sim 0.8\, v_f^{min} \sigma_R^* = 64$ksi, and $v_f^{min} = v_f(1 - L_o / L) = 0.4$. The ribbons are also wound at 90° (i.e. around the pipe circumference, as displayed in fig. 10), therefore the shear stress τ=0 and $\sigma_w = \sigma_N = \sigma_Z$. The short term pipe axial weeping strength (point 1 on fig. 11a) is increased by a factor of 6. The short term weeping strength for the downhole tubing application (point 2), as well as for buried pipe application (point 4) are increased by a factor of 2. Only the short term weeping strength of the surface pipe application (point 3) remains the same.

More importantly, the long term performance of the invention is expected to be much better than current composite pipe. In this example, the hoop and axial moduli have been increased from E_θ = 19GPa and $E_Z = E_N$ = 14GPa to E_θ = 37.6 and $E_Z = E_N$ = 31 GPa respectively. The original service factor of 0.25, i.e. $\sigma_\theta(t=20yrs)=0.25\sigma_0(t< 1\ hr)$ is expected to increase roughly by E_Z (ribbon pipe)/E_Z (current pipe) ~ E_θ(ribbon pipe)/E_θ(current pipe) ~ 2, i.e. the service factor is 0.5. The long term weeping strength of current pipe is compared with expected long term weeping strength of the invention in fig. 11b. The improvement in long term performance of the invention versus state of the art composite pipe is a factor of 12 in the axial weeping strength (point 1 on fig. 11b); a factor of 4 for both downhole tubing and buried pipe applications (points 2 and 4 on fig. 11b); and a factor of 2 for surface pipe application (point 3) on fig. 11b.

B. Random Ribbon Distribution

New short-term failure envelope is shown on fig. 12a for a pipe fabricated with ribbon-like glass fibers with aspect ratio s=340 and volume fraction of 50%, as compared to current state of the art. The fiber, interface and matrix have same mechanical properties as for section A. In this case, $\sigma_L^* = 100$ ksi, $\sigma_N^* \sim 34$ ksi (see Table 16). The failure criterion is same as for section A. The short term pipe axial weeping strength $\sigma_w = \sigma_N = \sigma_Z$ (point 1 on fig. 12a) is increased by a factor of 3. The short term weeping strength for the downhole tubing application (i.e. point 2), as well as for buried pipe application (point 4) are increased by a factor of 0.33 and 2 respectively. The short term weeping strength of the surface pipe application (point 3) is decreased by 20%.

The long term weeping strength of current pipe is compared with expected long term weeping strength of the invention in fig. 12b. The new service factor is calculated as in section A and is 0.5. The improvement in long term performance of the invention versus

state of the art composite pipe is a factor of 6 in axial weeping strength; a factor of 2.5 for downhole tubing application (point 2 on fig. 12b); a factor of 4 for buried pipe application (point 4); and a factor of 1.5 for surface pipe application (point 3)

VI. Glass Ribbon Fabrication

The glass ribbons described in this patent can be fabricated in several ways. One approach which is used commercially is the utilization of a redraw process, where an oversize preform with desired section geometry is heated to its softening point and then pulled, see US patent 3,425,454, Feb. 4, 1969.

CLAIMS:

1. A reinforced composite tubular body comprising:

(a) a tubular polymeric matrix including a thermosetting polymer with tensile elongation to break less than 25%;

(b) a glass ribbon reinforcing strip embedded within said tubular polymeric matrix.

2. The tubular body of claim 1 wherein said reinforcing strip is helically wound about the longitudinal axis of said tubular body between 0°–90°.

3. The tubular body of claim 2 wherein said reinforcing strip is wound at an angle of about 90° with respect to the pipe axis.

4. The tubular body of claim 3 wherein said ribbons have width L and the distance, ℓ, between two axially adjacent ribbons is between 0 and $\frac{L}{2}$.

5. The tubular body of claim 3 wherein said ribbons have width L and the length L_O by which a layer is offset with respect to the radially adjacent layer is between $\frac{L}{10}$ and $\frac{L}{2.}$

6. The tubular body of claim 1 wherein said glass ribbon reinforcing strip has an aspect ratio s, a critical aspect ratio, s_c, such that $\frac{s}{s_c} \geq 1$.

7. The tubular body of claim 1 wherein the transverse Young's modulus is greater than 50% of the rule of mixture value.

8. The tubular body of claim 1 wherein the interfacial shear strength, τ_i, is greater than or equal to 2 ksi.

9. The tubular body of claim 1 wherein the epoxy tensile strength, σ_m, is equal to or greater than the interfacial shear strength, τ_i.

10. The tubular body of claim 6 wherein said glass ribbon reinforcing strip has an aspect ratio s, a critical aspect ratio, s_c, such that $\frac{s}{s_c} \leq 5$.

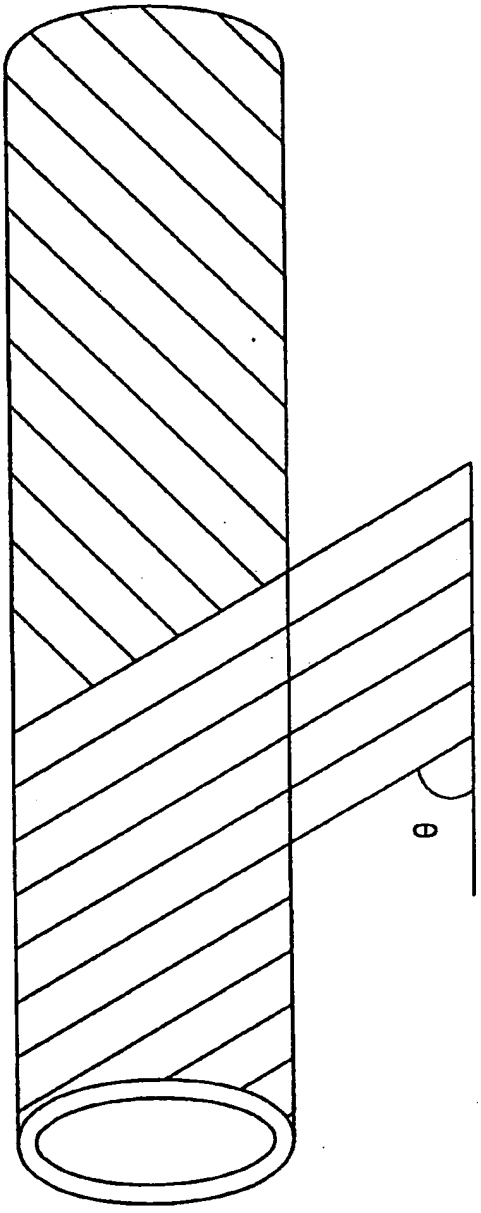

EXAMPLE PIPE / TUBULAR FOR FLUID CONTAINMENT. THE WINDING ANGLE θ = 55°, AND THE FIBER VOLUME FRACTION IS ABOUT 60%

FIG. 1

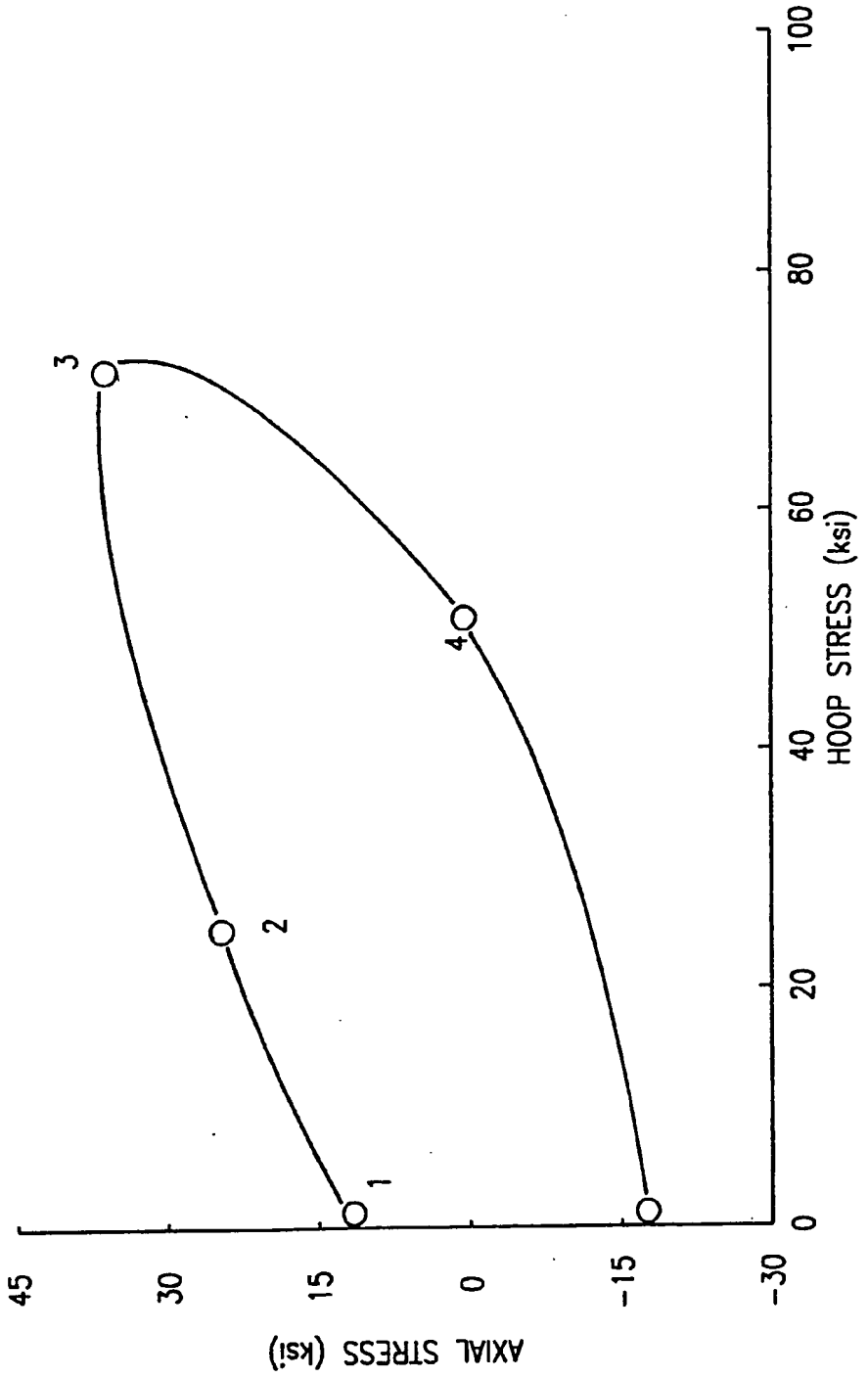
AXIAL STRESS (ksi)
45
30
15
0
-15
-30
HOOP STRESS (ksi)
0
20
40
60
80
100
1
2
3
4

FIG. 2

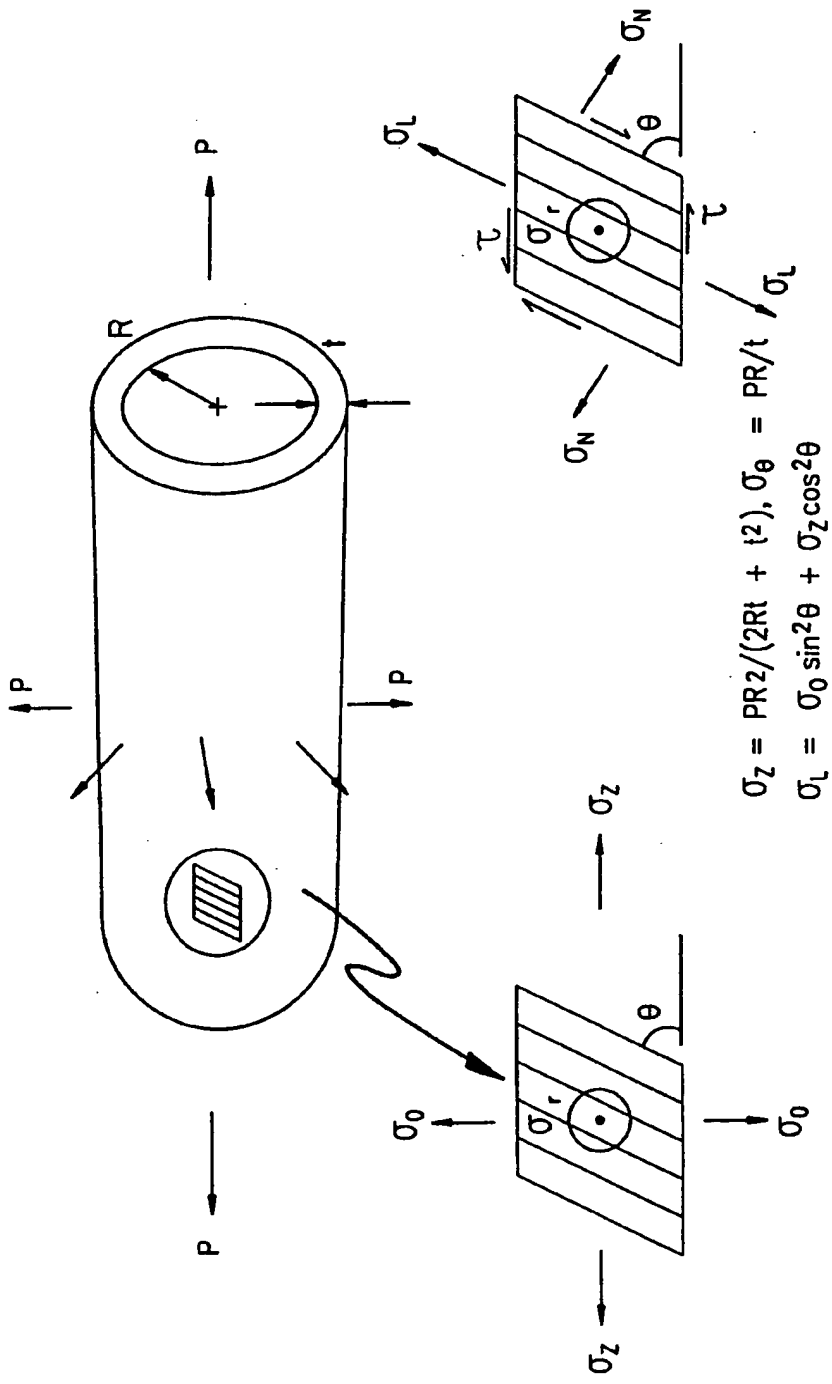

LOCAL STRESSES INDUCED BY FLUID PRESSURE ON A VOLUME ELEMENT OF LAMINATE FORMING THE PIPE WALL. THE WINDING ANGLE IS $\theta = 55°$

FIG. 3

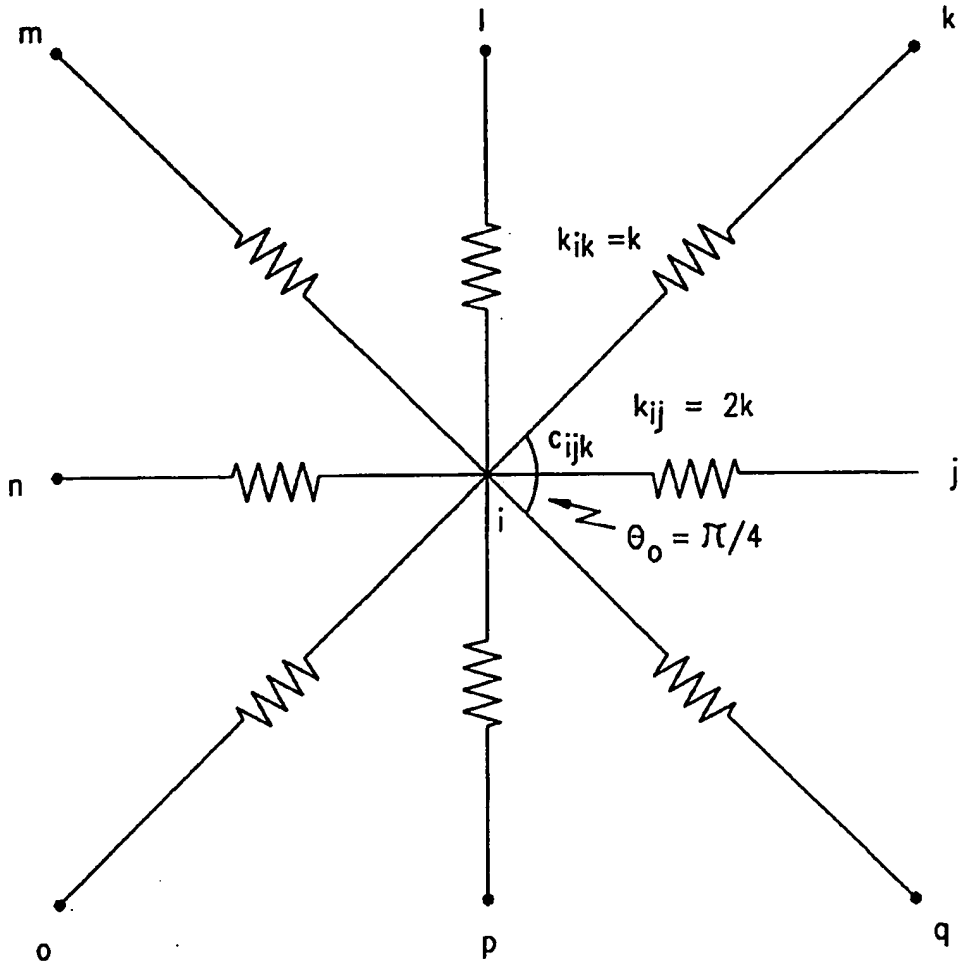

FIG. 4

FIG. 5

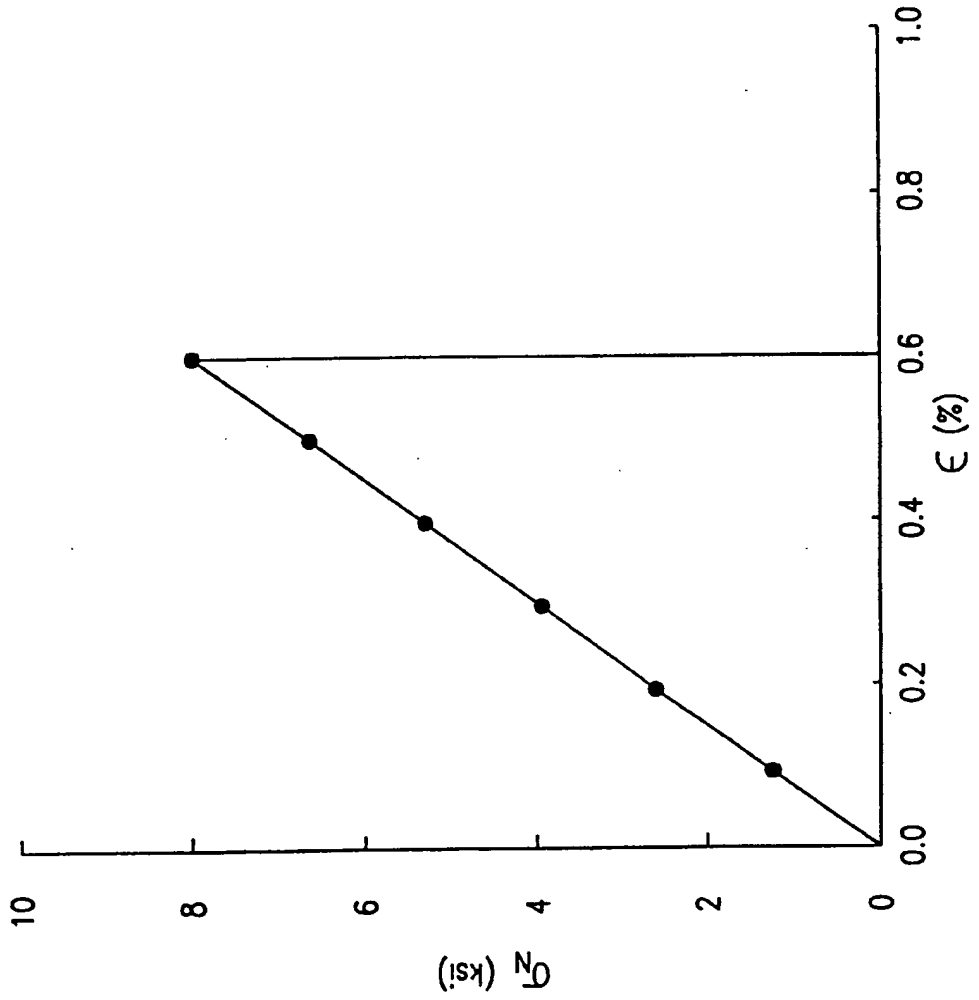

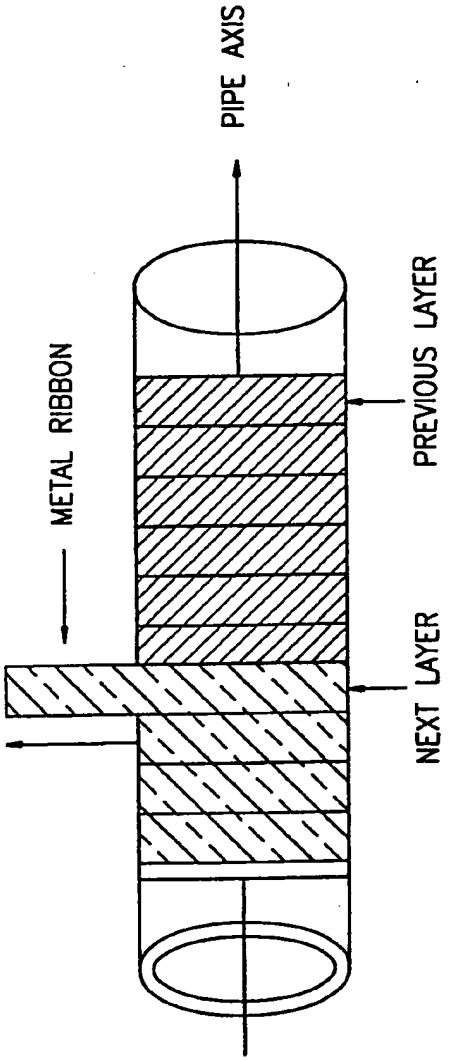
PIPE AXIS
METAL RIBBON
PREVIOUS LAYER
NEXT LAYER

FIG. 6a

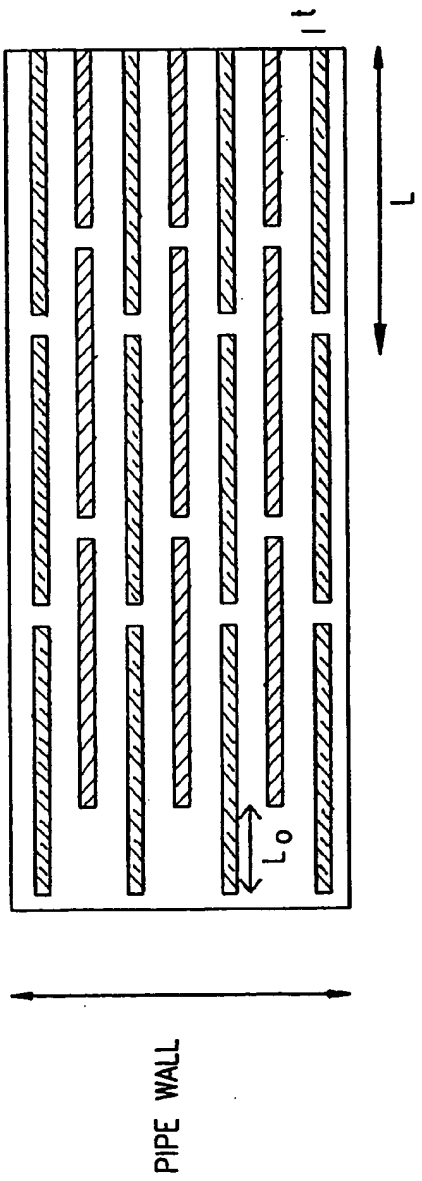
RIBBON TRANSVERSE ASPECT RATIO S=L/t
t
L
L_o
PIPE WALL

FIG. 6b

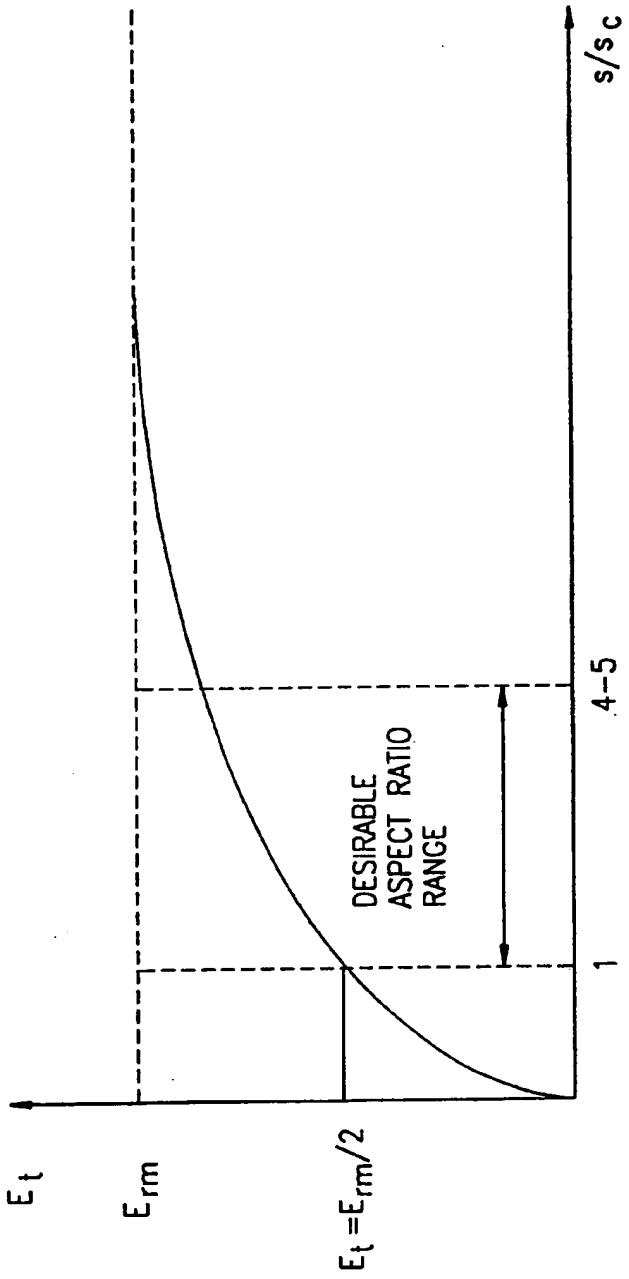

FIG. 7

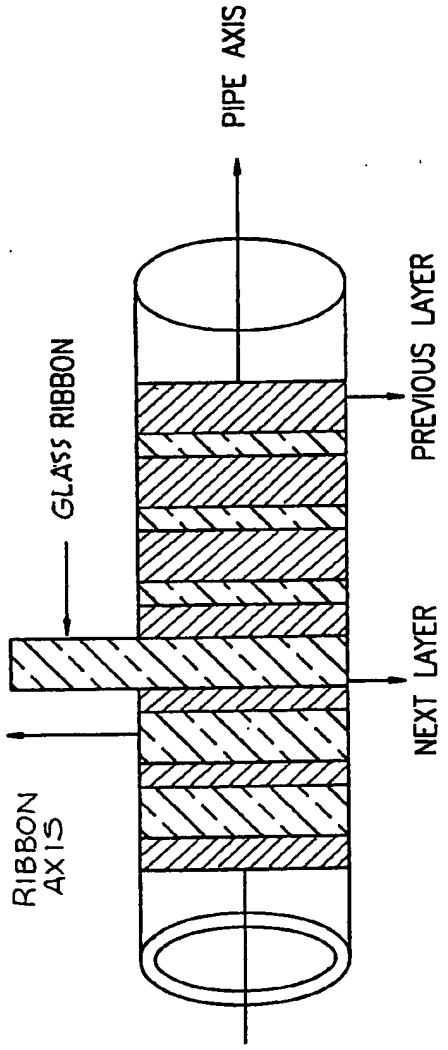
PIPE AXIS
GLASS RIBBON
PREVIOUS LAYER
NEXT LAYER
RIBBON AXIS

FIG. 8a

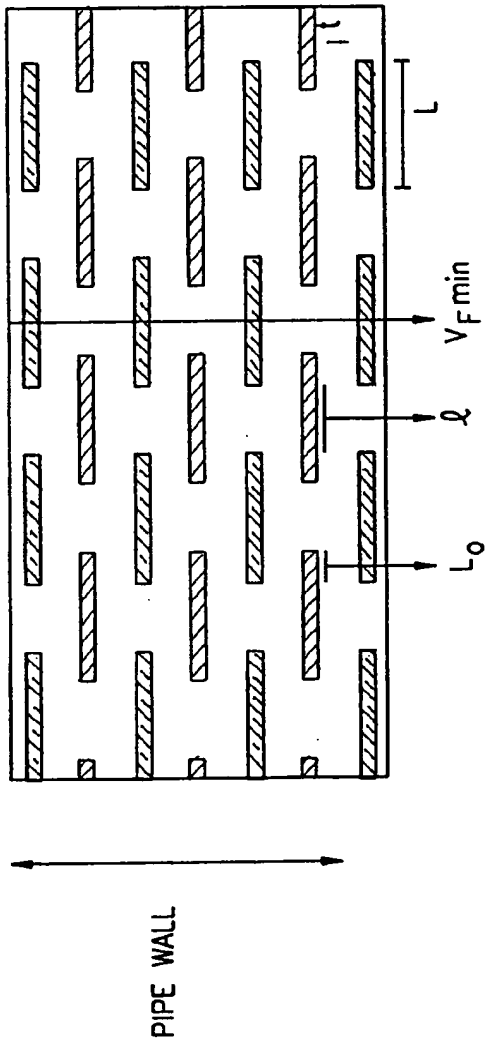
RIBBON TRANSVERSE ASPECT RATIO S=L/t
t
L
V_F min
ℓ
L_o
PIPE WALL

FIG. 8b

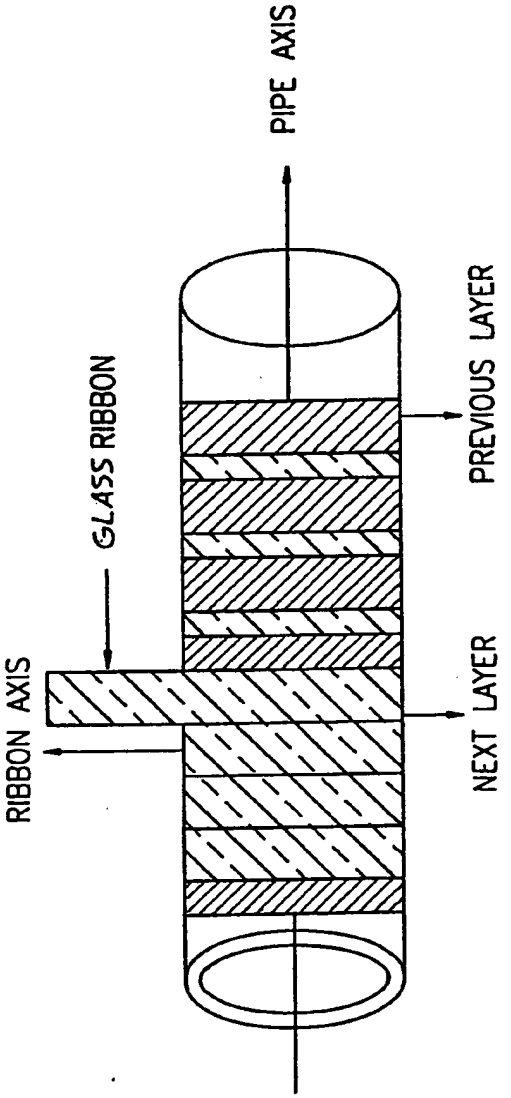
PIPE AXIS
GLASS RIBBON
PREVIOUS LAYER
RIBBON AXIS
NEXT LAYER

FIG. 9a

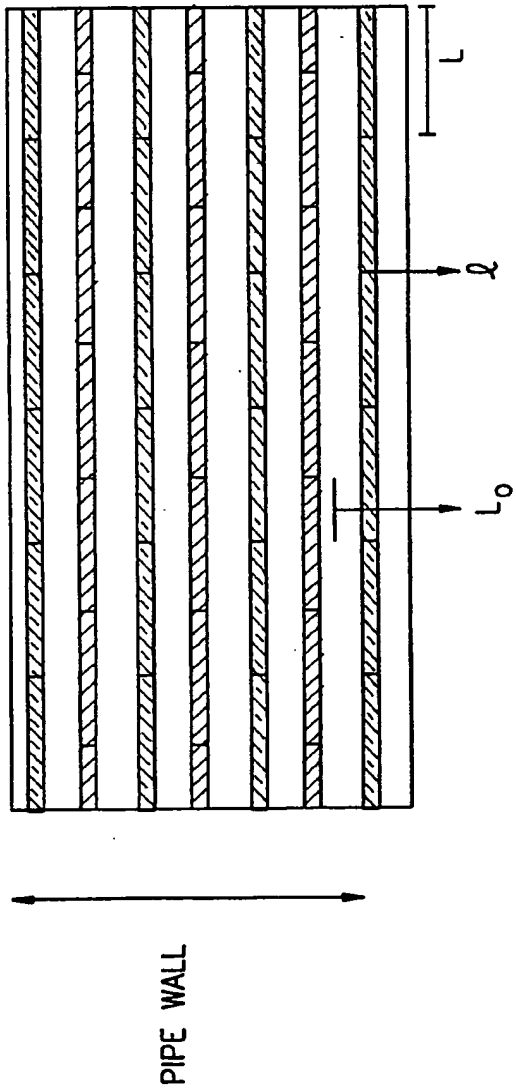
RIBBON TRANSVERSE
ASPECT RATIO S=L/t
t
L
l
L_o
PIPE WALL

FIG. 9b

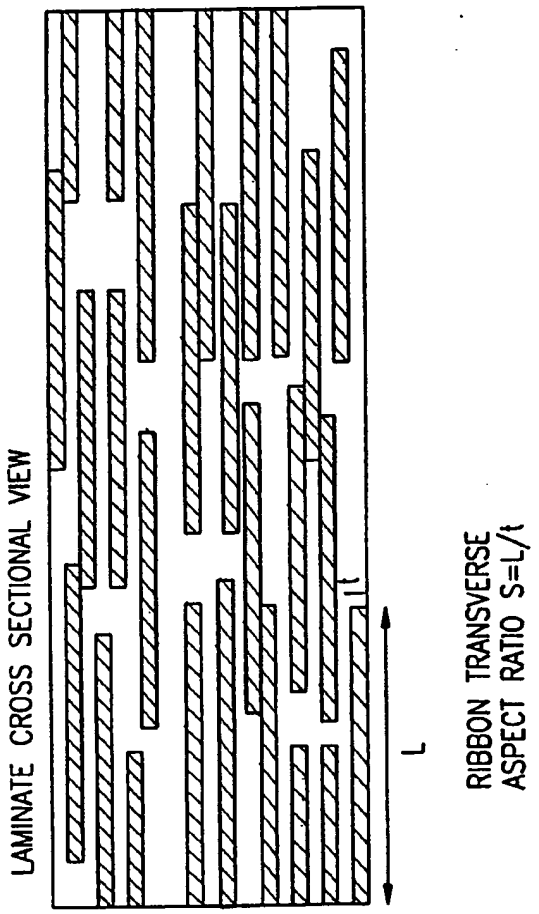

FIG. 10b

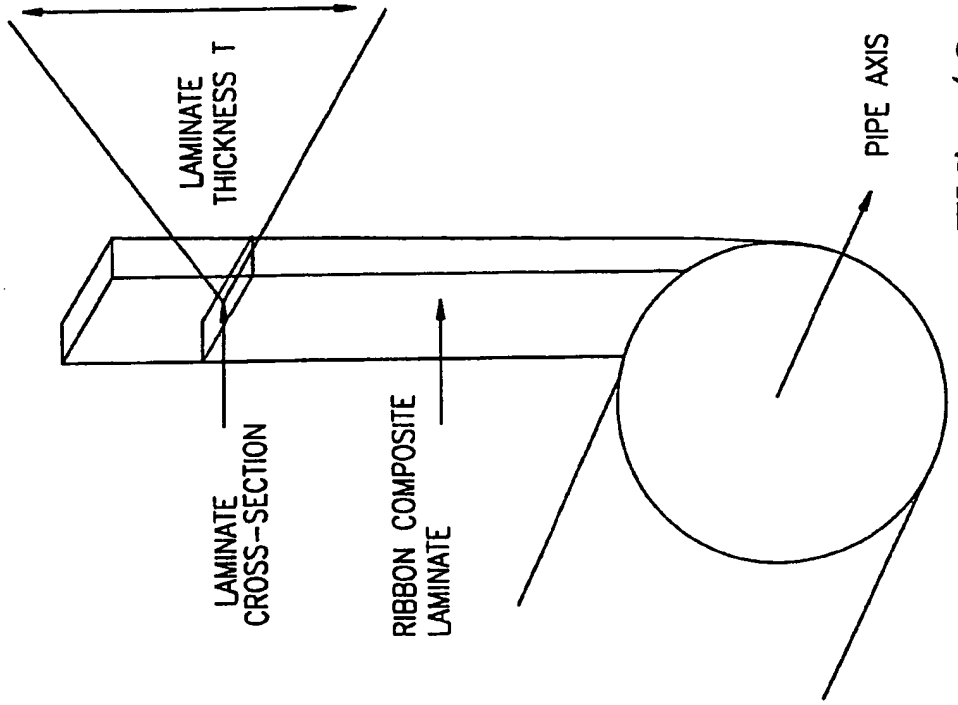

FIG. 10a

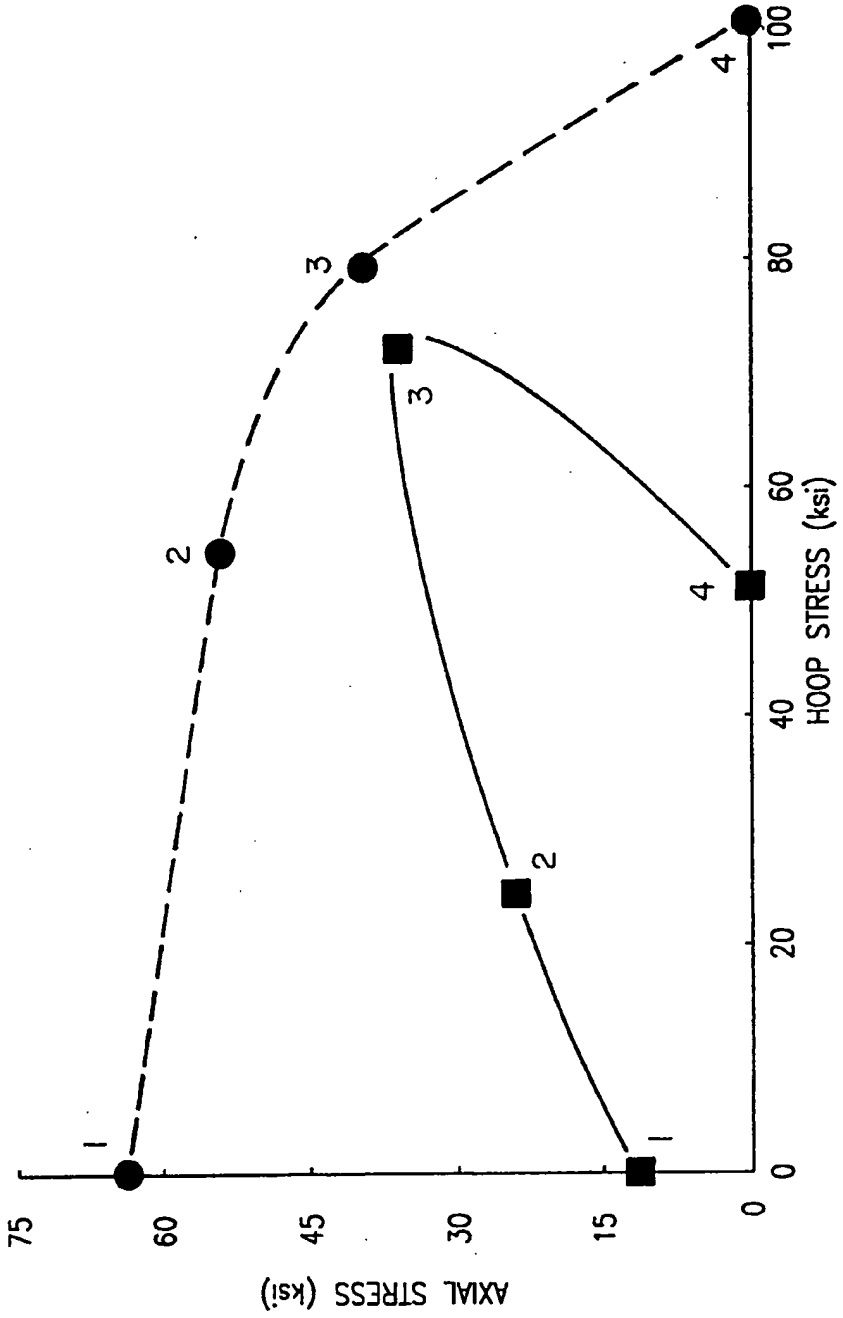
AXIAL STRESS (ksi)
75
60
45
30
15
0
HOOP STRESS (ksi)
0
20
40
60
80
100
1
2
3
4
1
2
3
4

FIG. 11a

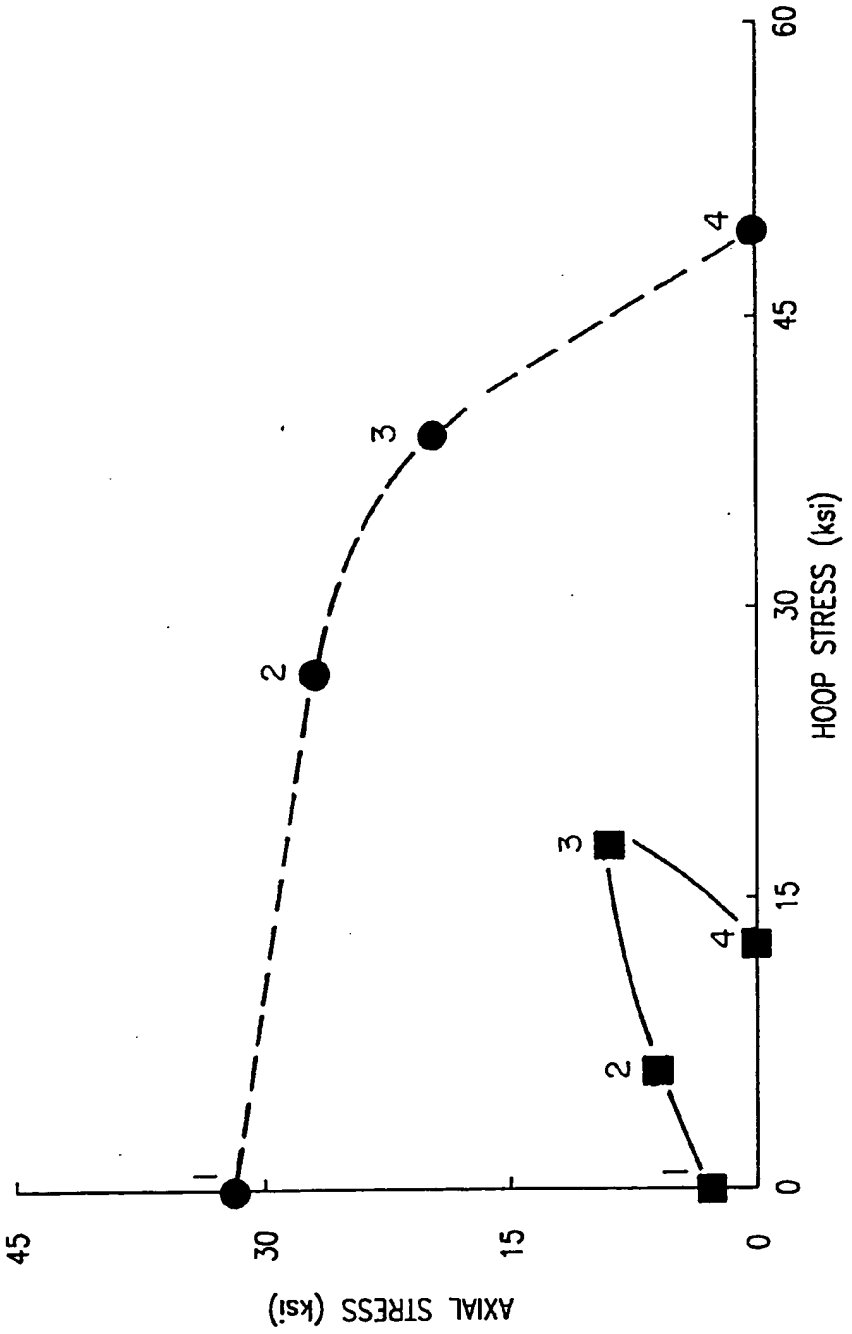
AXIAL STRESS (ksi)
45
30
15
0
HOOP STRESS (ksi)
60
45
30
15
0
1
2
3
4
1
2
3
4

FIG. 11b

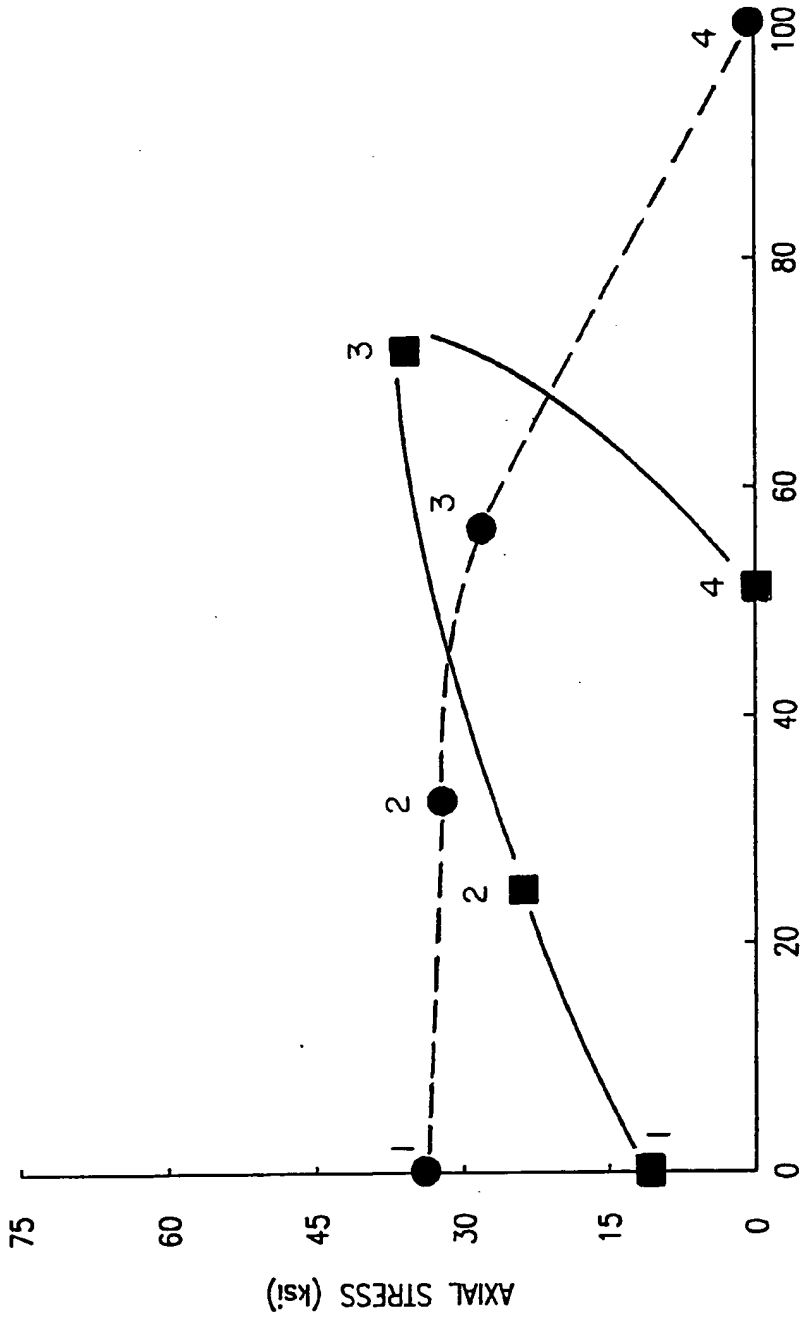
AXIAL STRESS (ksi)
75
60
45
30
15
0
HOOP STRESS (ksi)
0
20
40
60
80
100
1
2
3
4

FIG. 12a

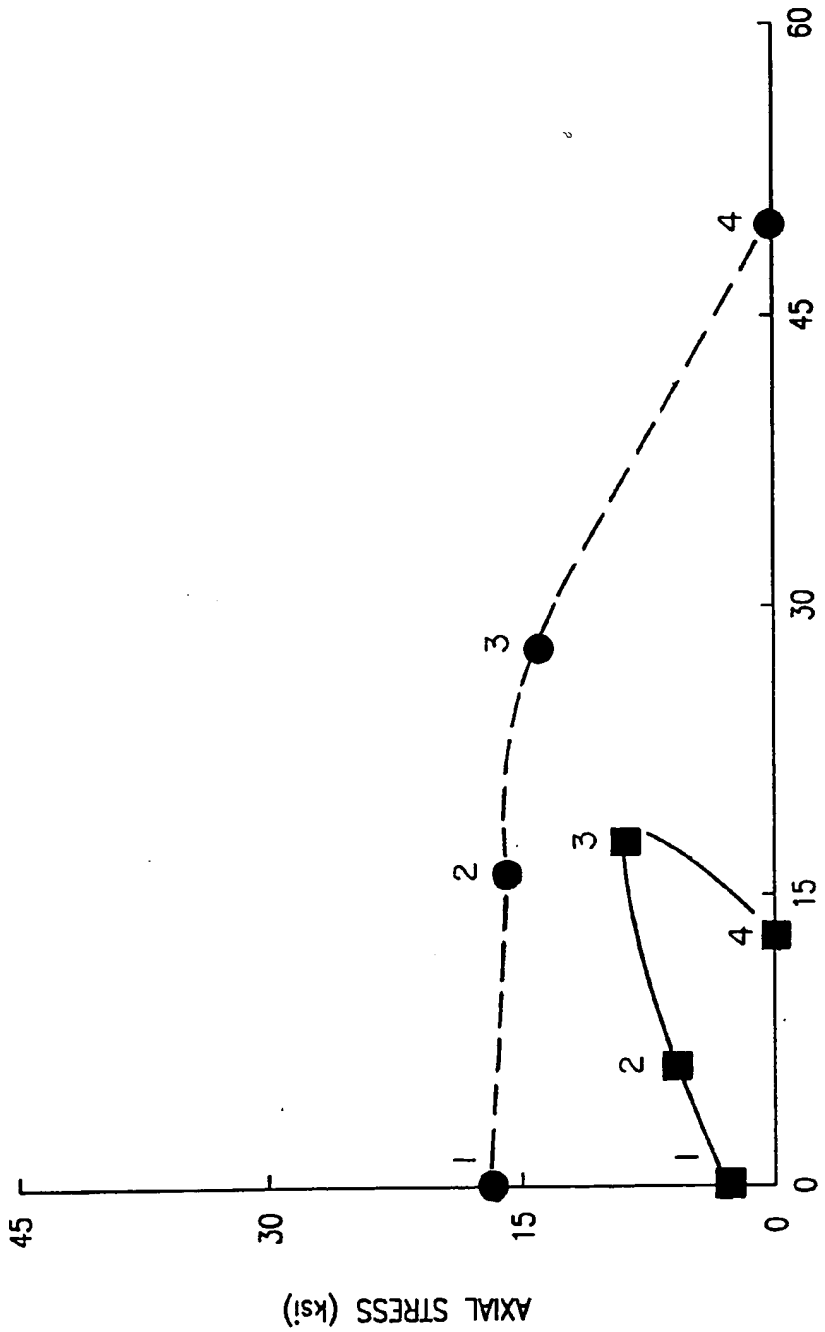
HOOP STRESS (ksi)
0
15
30
45
60
AXIAL STRESS (ksi)
0
15
30
45
1
2
3
4
1
2
3
4

FIG. 12b

INTERNATIONAL SEARCH REPORT

International application No.
PCT/US97/13342

A. CLASSIFICATION OF SUBJECT MATTER
IPC(6) :F16L 9/14
US CL : 138/153
According to International Patent Classification (IPC) or to both national classification and IPC

B. FIELDS SEARCHED

Minimum documentation searched (classification system followed by classification symbols)

U.S. : 138/153, 125, 132, 174, dig 2

Documentation searched other than minimum documentation to the extent that such documents are included in the fields searched

Electronic data base consulted during the international search (name of data base and, where practicable, search terms used)

C. DOCUMENTS CONSIDERED TO BE RELEVANT

Category*	Citation of document, with indication, where appropriate, of the relevant passages	Relevant to claim No.
Y	US 2,467,999 A (STEPHENS) 19 April 1949, see entire document.	1-10
Y	US 2,888,042 A (ST. JOHN et al) 26 May 1959, see entire document.	1-10
Y	US 3,350,030 A (GREEN) 31 October 1967, see entire document.	1-10
Y	US 3,447,572 A (VANDERBILT et al) 03 June 1969, see entire document.	1-10
Y	US 4,243,075 A (MCPHERSON et al) 06 January 1981, see entire document.	1-10
Y	US 5,324,558 A (MUTO et al) 28 June 1994, see entire document.	1-10

☐ Further documents are listed in the continuation of Box C. ☐ See patent family annex.

*	Special categories of cited documents:	"T"	later document published after the international filing date or priority date and not in conflict with the application but cited to understand the principle or theory underlying the invention
"A"	document defining the general state of the art which is not considered to be of particular relevance	"X"	document of particular relevance; the claimed invention cannot be considered novel or cannot be considered to involve an inventive step when the document is taken alone
"B"	earlier document published on or after the international filing date	"Y"	document of particular relevance; the claimed invention cannot be considered to involve an inventive step when the document is combined with one or more other such documents, such combination being obvious to a person skilled in the art
"L"	document which may throw doubts on priority claim(s) or which is cited to establish the publication date of another citation or other special reason (as specified)	"&"	document member of the same patent family
"O"	document referring to an oral disclosure, use, exhibition or other means		
"P"	document published prior to the international filing date but later than the priority date claimed		

Date of the actual completion of the international search 14 SEPTEMBER 1997	Date of mailing of the international search report 24 OCT 1997
Name and mailing address of the ISA/US Commissioner of Patents and Trademarks Box PCT Washington, D.C. 20231 Facsimile No. (703) 305-3230	Authorized officer for JAMES F. HOOK Telephone No. (703) 308-0861

Form PCT/ISA/210 (second sheet)(July 1992)*